Bioorganic Chemistry 153 (2024) 107917

Contents lists available at ScienceDirect

Bioorganic Chemistry

journal homepage: www.elsevier.com/locate/bioorg

"Novel chemo-enzymatic synthesis, structural elucidation and first antiprotozoal activity profiling of the atropoisomeric dimers of *trans*-8-Hydroxycalamenene"

Ivan Bassanini [a,*], Chiara Tognoli [a], Massimiliano Meli [a], Silvia Parapini [b], Nicoletta Basilico [c], Giovanni Fronza [d], Stefano Serra [d], Sergio Riva [a]

[a] *Istituto di Scienze e Tecnologie Chimiche ''Giulio Natta'' – SCITEC, Consiglio Nazionale delle Ricerche, Via Mario Bianco 9, 20131 Milano, Italy*
[b] *Dipartimento di Scienze Biomediche per la Salute, Università degli Studi di Milano, Via Pascal 36, 20133, Milano, Italy*
[c] *Dipartimento di Scienze Biomediche, Chirurgiche ed Odontoiatriche, Università degli Studi di Milano, Via Pascal 36, 20133, Milano, Italy*
[d] *Istituto di Scienze e Tecnologie Chimiche ''Giulio Natta''– SCITEC, Consiglio Nazionale delle Ricerche, Via Luigi Mancinelli 7, 20131, Milano, Italy*

ARTICLE INFO

Keywords:
Calamenene
Terpenes
Metabolites
Biocatalysis
Trametes versicolor laccase
Leishmaniasis
Plasmodium falciparum Malaria

ABSTRACT

Leishmaniasis and malaria are two debilitating protozoan diseases affecting millions globally, particularly in tropical and subtropical regions. Current therapeutic options face significant challenges due to emerging drug-resistant strains, necessitating the discovery of novel antiprotozoal agents. This study explores, for the first time, the antiprotozoal potential of calamenenes and their dimers, naturally occurring sesquiterpenes found in essential oils, through a novel chemo-enzymatic synthesis approach. Using the laccase from *Trametes versicolor*, atropoisomeric dimers of (−)- and (+)-8-*trans*-hydroxycalamenene were synthesized from commercially available (−)- and (+)-menthol. Structural elucidation was achieved via 2D-NMR spectroscopy, electronic circular dichroism, and DFT calculations. *In vitro* profiling against *Leishmania* spp and drug-resistant *Plasmodium falciparum* revealed that calamenene dimers exhibited significantly higher antiprotozoal activity compared to their monomeric counterparts, highlighting the potential of dimeric terpenoids as promising antiprotozoal agents. This work lays the foundation for developing novel antimalarial drugs based on calamenene scaffolds, encouraging further interactome studies to optimize their pharmacological properties.

1. Introduction

Leishmaniasis and malaria are two protozoan diseases affecting millions of people worldwide, particularly in tropical and subtropical regions. Leishmaniasis, caused by the *Leishmania* parasite, manifests in various forms, ranging from cutaneous lesions to potentially fatal visceral infections [1]. Malaria, on the other hand, is caused by *Plasmodium* parasites, with *P. falciparum* (*P.f.*) being the most lethal strain, responsible for severe illness and high mortality rates. [2] These human parasitosis, have respectively caused more than 600 000 deaths (76 % of them are children aged under 5 years) and an estimated number of 700 000 to 1 million new cases worldwide, according to the World Health Organization (WHO) annual reports for 2023 [3,4].

Despite ongoing efforts to control and treat these diseases, current therapeutic options face significant challenges as drug-resistant strains diminish their efficacy and long-term sustainability. Accordingly, to outpace the evolving resistance patterns of protozoan parasites, an urgent need of novel antiprotozoal agents with unique mechanisms of action or biological targets is currently emerging [5–10]. In this framework, different strategies of drug design and development have been explored by our group comprising the repositioning or repurposing of FDA-approved drugs, [11,12] the rational design of protein-targeting antiprotozoal candidates [13,14] and the *de-novo* investigation of chemotypes never reported as antiprotozoal pharmacophores (Fig. 1) [15–17].

The exploration of what Nature has to offer has largely inspired medicinal chemists during the scaffold hopping stage, since the structural complexity of the natural products (NP) represents a treasure in

* Corresponding author.
E-mail addresses: ivan.bassanini@cnr.it (I. Bassanini), chiara.tognoli@scitec.cnr.it (C. Tognoli), massimiliano.meli@scitec.cnr.it (M. Meli), silvia.parapini@unimi.it (S. Parapini), nicoletta.basilico@unimi.it (N. Basilico), giovanni.fronza@scitec.cnr.it (G. Fronza), stefano.serra@scitec.cnr.it (S. Serra), sergio.riva@scitec.cnr.it (S. Riva).

https://doi.org/10.1016/j.bioorg.2024.107917
Received 25 September 2024; Received in revised form 18 October 2024; Accepted 22 October 2024
Available online 24 October 2024

terms of biodiversity [18].

Terpenes, a diverse class of NP produced by plants, fungi, and marine organisms, are crucial players of many biological processes *in vivo* and serve as precursors to various bioactive molecules [19–21]. Among them, calamenenes and their hydroxylated metabolites (Fig. 2a) are representative bioactive sesquiterpenes found in several essential oils of different plant sources and often associated with diverse biological activities, from antioxidant to antiproliferative and anticancer [22–33].

Interestingly, calamenenes-containing essential oils have been related also with antiprotozoal activities highlighting how calamenene skeleton could represent a natural product lead for the development of novel antiprotozoal agents [34–39]. However, dose–response studies on isolated calamenenes were rarely conducted as only essential oils (or calamenenes-enriched derivatives of them) were usually screened *in vitro* [38]. Moreover, stereochemical indications were generally missing [38,40]. In addition, as highlighted by recent studies, the dimerization of NP (either natural or synthetically induced) offers an easy entry to novel compounds potentially endowed with unique biological profiles as structural modifications can significantly influence their interaction with biological target(s) as well as their pharmacokinetic properties [41–44]. Interestingly, only few reports dealing with dimeric calamenenes, usually referred as bicalamenenes, can be found in the literature (Fig. 2b) and their biological profiles remain practically unknown [32,33,40,45,46].

In this scenario, we got interested in the possibility of proposing a convenient synthetic entry to bicalamenenes, scaffolds that exist in the peculiar form of stable atropisomers [40,45,46]. Moreover, considering the lack of specific dose–response studies regarding the antiprotozoal activity of calamenene terpenoids, a detailed *in vitro* profiling of the growth inhibitory activity of both the parental calamenenes and their corresponding dimers against parasite culture of *Leishmania* spp and *P.f.* was programmed.

Accordingly, a novel chemoenzymatic synthesis of the dimers of (−)- and (+)-8-*trans*-hydroxy calamenene (8-*trans*-HC) was built starting from commercially available (−)- and (+)-menthol (Scheme 1). Briefly, (−)- and (+)-menthol were respectively converted into (−)- and (+)-8-*trans*-HC following a synthetic protocol previously reported by us [47], and based on the benzannulation of substituted 3-alkoxycarbonyl-3,5-hexadienoic acids as a key step [48]. Then, the laccase from *Trametes versicolor* (*TvLac*), an enzyme able to activate normally inert Csp^2-H bonds at the expense of molecular oxygen [49,50], allowed the easy preparation of the target compounds *via* the oxidative dimerization of the two substrates. Finally, the target products were structurally and biologically characterized.

2. Materials and methods

2.1. General

Abbreviations used: DCM: dichloromethane; AcOEt = ethyl acetate; TMEDA: *N,N,N′,N′*-tetrametil-etilendiammina; r.t. = room temperature; DMF = *N,N*-Dimethylformamide; THF = Tetrahydrofuran; TEA = triethylamine; DMSO = dimethyl sulfoxide; *TvLac* = *Trametes versicolor* laccase; TLC = thin-layer chromatography; isolated yield: isolated yield; C_6D_6 = Deuterated benzene; DFT = Density Functional Theory; EDC = Electronic Circular Dichroism; SI = Supporting Information; Rt = Retention factor; t_R = Retention time.

All solvents and reactants, and the enzyme were purchased from Sigma-Aldrich (St. Louis, MO, USA) whereas (+)-menthol was purchased from TCI Europe N.V. (Zwijndrecht, Belgium).

The laccase from *Trametes versicolor* (*TvLac*) was purchased from Sigma-Aldrich. The enzyme activity was evaluated according to literature assay based on ABTS (2,2′-azino-bis(3-ethylbenzothiazoline-6-sulfonic acid)) as model substrate [51].

Biotransformations were performed in a G24 Environmental Incubator New Brunswick Scientific Shaker (Edison, USA) or in a Thermomixer Comfort (Eppendorf, DE). Flash column chromatography was performed on a silica gel 60 (70–230 mesh, Merck, DE).

Novel compounds were characterized by ^{1}H- and ^{13}C NMR, HR-mass spectrometry, and, when necessary, by measuring their optical rotation values. The structures of the compounds previously reported in the literature were confirmed by comparing their ^{1}H spectra and HR mass spectra with reported data.

^{1}H- and ^{13}C NMR spectra were recorded at 24 °C degrees with a

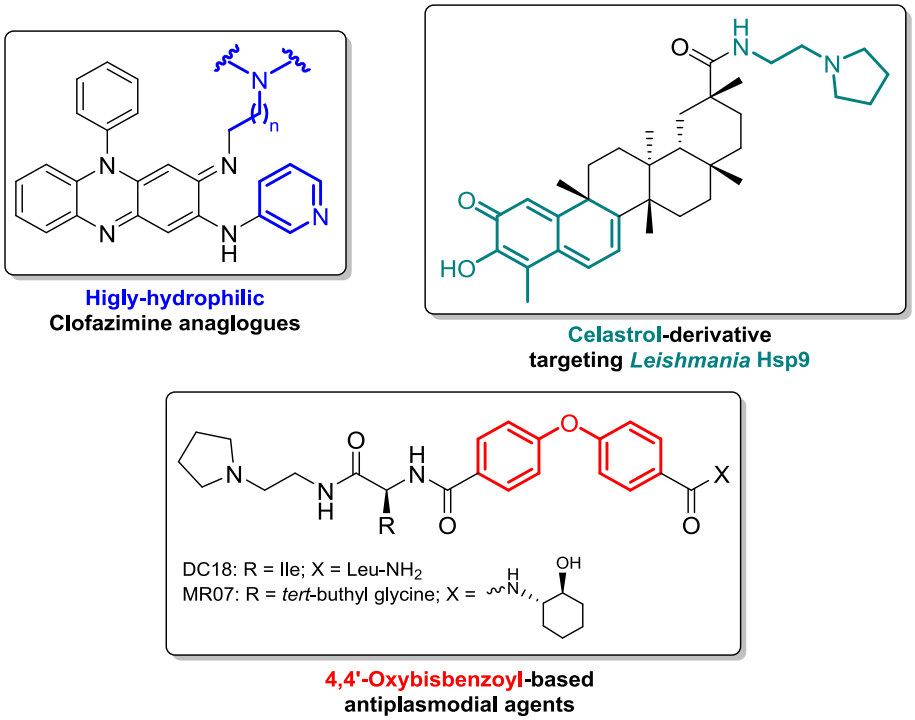

Fig. 1. Examples of the antiprotozoal candidates developed by our research group through the years. [11–17].

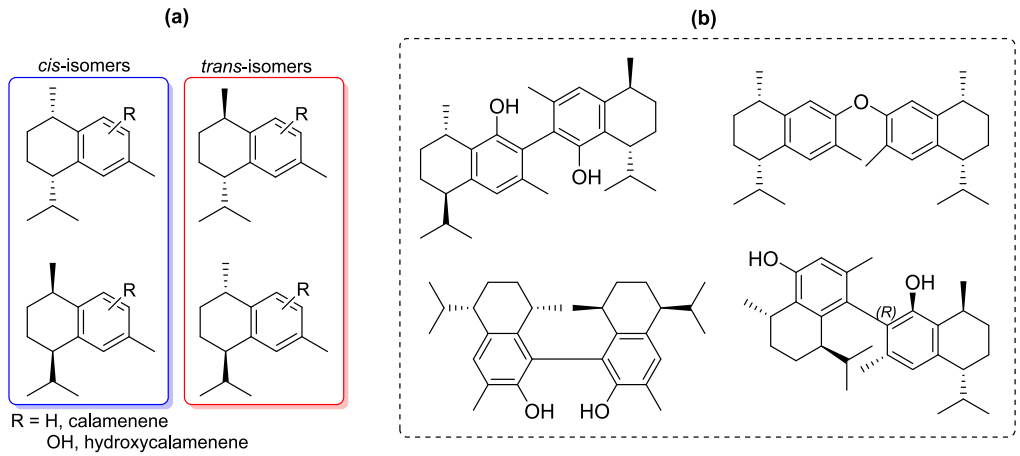

Fig. 2. (a) Structures and stereoisomers of calamenene and their hydroxylated metabolites; (b) Literature-reported hydroxycalamenene dimers. [33,40,45,46].

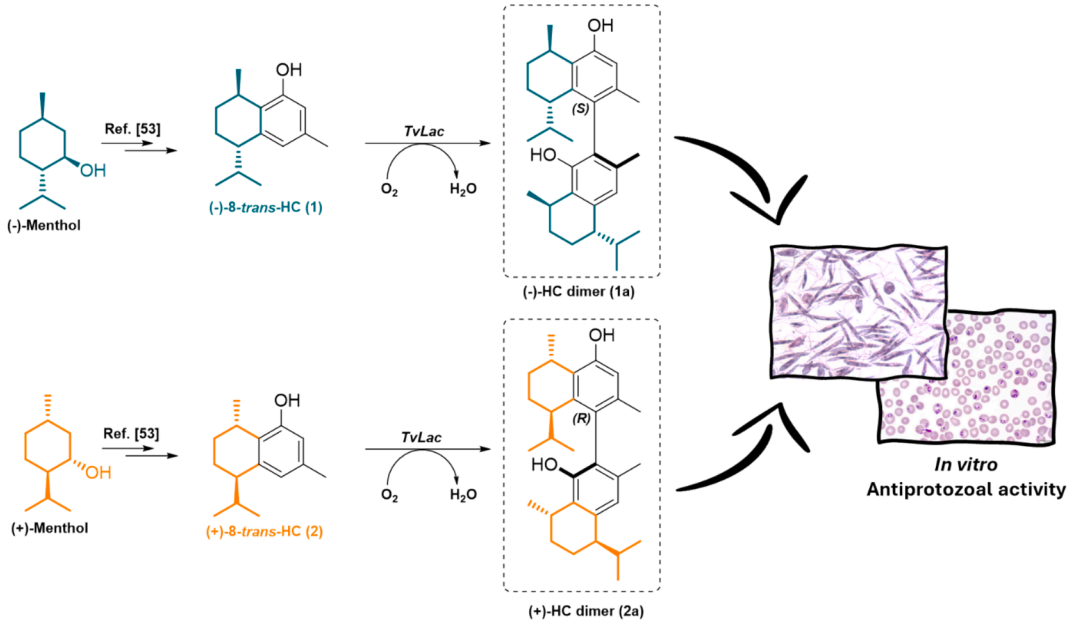

Scheme 1. A novel chemoenzymatic entry to 8-*trans*-HC dimers as potential antiprotozoal agents.

Bruker Avance spectrometer (400 MHz) in $CDCl_3$.

High-resolution mass spectra (HRMS) were conducted on FT-Orbitrap mass spectrometer in positive electrospray ionization (ESI).

Optical rotations were measured in a 1.0 cm tube with a Jasco P-2000 polarimeter.

Electronic circular dichroism spectra were recorded on a nitrogen flushed Jasco J-1100 spectropolarimeter (Easton MD, USA) interfaced with a thermostatically controlled cell holder. The analyses were performed in the range between 200 and 400 nm at 25 °C in quartz cuvettes. The purified compounds were dissolved in methanol (0.15 mg mL^{-1} final concentration).

GC–MS analyses were performed using an HP-6890 gas chromatograph equipped with a 5973 mass detector and using an *HP-5MS* column (30 m × 0.25 mm, 0.25 μm film thickness; Hewlett Packard, Palo Alto, CA, USA) used with the following temperature program: 60° (1 min)–6°/min–150° (1 min)–12°/min–280° (5 min); carrier gas: He; constant flow 1 mL/min; split ratio, 1/30; t_R given in minutes.

Reactions were monitored by TLC of precoated silica gel 60 matrix with fluorescent indicator 254 nm on Al foils analyzed with UV lamp or developed with the Komarovsky reagent (p-hydroxybenzaldehyde 15 g, H_2SO_4 50 % 100 mL, MeOH 1 L) or the phosphomolybdic reagent ($(NH_4)_6MoO_4$ 42 g, $Ce(SO_4)_2$ 2 g, H_2SO_4 62 mL, H_2O 1 L).

2.2. Synthetic chemistry

2.2.1. Preparation of (+)-8-trans-HC

(+)-Menthone ***(i)***. To a mechanically stirred solution of (+)-menthol (50 g, 320 mmol) in diethyl ether (350 mL) Jones reagent (sulfuric acid-chromium trioxide mixture, 1.65 eq) was added dropwise, maintaining the temperature of the mixture below 25 °C with the aid of an ice bath. After completion of the reaction (by TLC analysis, 2 h), the organic layer was separated, and the aqueous one extracted with diethylether. The combined organic phases were washed with a saturated solution of $NaHCO_3$, dried over anhydrous Na_2SO_4 and evaporated under reduced pressure. The residue obtained was distilled at reduced pressure to afford the pure **(i)** (37 g, 240 mmol, 75 % yield) as a colorless oil.

^{1}H NMR (400 MHz, $CDCl_3$) δ 3.42 (td, J = 10.5, 4.3 Hz, 1H), 2.25–2.14 (m, 1H), 2.01–1.83 (m, 1H), 1.75–1.64 (m, 1H), 1.64–1.59 (m, 1H), 1.58–1.34 (m, 2H), 1.18–1.07 (m, 1H), 1.03–0.95 (m, 2H), 0.93 (dd, J = 9.3, 6.8 Hz, 6H), 0.89 – 0.84 (m, 1H), 0.82 (d, J = 7.0 Hz, 3H). ^{13}C NMR (100 MHz, $CDCl_3$) δ 71.52, 50.14, 45.06, 34.55, 31.64, 25.82, 23.14, 22.21, 21.01, 16.09. $[\alpha]_D$ (*c* 0.5, $CHCl_3$): +27.6. Data in

agreement with literature values [52].

*Aldehyde **(ii)**. (a)* Intermediate (**i**) (1.0 eq, 2.3 M in DCM) was slowly added to an ice-cooled, mechanically stirred DCM suspension of *p*-toluenesulfonyl hydrazine (0.74 eq), and the mixture was stirred for approximately 2 h at 0 °C. Hence, the reaction was diluted with the same volume of hexane and then was slowly concentrated under reduced pressure using a rotavapor equipped with a cooled bath (0–10 °C). When almost all solvent was removed the hydrazone start to precipitate. This material was suspended in hexane, was cooled (0 °C), filtered on a Buchner funnel and the filtrate was washed with cold hexane.

(b) The obtained hydrazone was suspended in a 2:1 mixture of hexane/TMEDA (1.2 M, 1.0 eq) and was cooled to −78 °C. Then, the reaction was mechanically stirred and a hexane solution of BuLi (2.5 M, 5.0 eq) was added dropwise, under nitrogen atmosphere. The mixture was stirred for 10 min at −78 °C and then allowed to warm to r.t. for one additional hour (nitrogen evolution occurred at temperature superior to 0 °C). Hence, the mixture was cooled again at −78° C and DMF (10 eq) was added. The reaction was left to reach room temperature and finally was quenched with saturated aqueous NH_4Cl and extracted with a 1:1 (v/v) mixture of hexane and diethyl ether. The combined organic layers were dried over anhydrous Na_2SO_4 and evaporated under reduced pressure. The residue obtained was purified by silica gel column chromatography (hexane:AcOEt, from 100:0 to 90:10) and distilled affording pure **(ii)** as an oil (55 % isolated yield).

^{1}H NMR (400 MHz, $CDCl_3$) δ 9.32 (s, 1H), 6.64 – 6.51 (m, 1H), 2.49 – 2.18 (m, 3H), 1.88 – 1.70 (m, 2H), 1.61 (dtd, J = 13.5, 6.7, 3.4 Hz, 1H), 1.49 – 1.29 (m, 1H), 1.03 (d, J = 7.3 Hz, 3H), 0.84 (d, J = 7.0 Hz, 3H), 0.62 (d, J = 6.9 Hz, 3H). ^{13}C NMR (400 MHz, $CDCl_3$) δ 194.4,158.3, 143.8, 37.6, 31.4, 28.7, 27.9, 20.6, 20.6, 20.5, 17.0. EI-MS *m/z* 166 (61), 151 (11), 137 (12), 123 (100), 109 (49), 95 (74), 81 (36), 67 (23). $[\alpha]_D$ (*c* 3, $CHCl_3$): −89.8.

*Phenol **(iii)**. (a)* LDA (15 mL of a 2 M solution in THF) was added dropwise, under a static atmosphere of nitrogen, to a cooled (−60 °C) solution of dimethyl succinate (3,9 g, 26.7 mmol) in dry THF (15 mL). After 10 min, aldehyde **(ii)** (4 g, 24.1 mmol) in dry DMPU (4 mL) was added dropwise and the reaction was stirred for 1 h. Hence, additional LDA (12.1 mL of a 2 M solution in THF) was introduced, and the mixture was left to reach r.t (24 °C). The progress of the reaction was checked by TLC observing the aldehyde concentration decreasing and the formation of a dienic acid. When the transformation didn't proceed any longer (2 h), the mixture was quenched with saturated aqueous NH_4Cl, acidified with diluted HCl aq. and extracted with ethyl acetate. The combined organic layers were washed with brine, dried over anhydrous Na_2SO_4 and evaporated under reduced pressure. The residue was made up of a mixture of the product ***iii***, unreacted aldehyde ***ii*** unreacted dimethyl succinate, and a minority amount of the dienic acid isomers, namely the 3-(Z) and the 2,5-dienoic acid isomers. Since the chromatographic separation of the dienoic acid isomers was unsuccessfully and only 3-(*E*)-hexadienoic acid can give benzannulation reactions, the crude reaction mixture was used as such in the next step.

(b) The obtained crude reaction mixture was taken-up in dry THF (30 mL), TEA (15 mL) was added, and the mixture was cooled with an ice-bath. Trifluoroacetic anhydride (5 mL, 36 mmol) was then added dropwise under magnetic stirring and the mixture was allowed to warm to r.t. Stirring was prolonged for 1 h, then the reaction was acidified with diluted HCl aq. and extracted with AcOEt. The combined organic layers were dried over anhydrous Na_2SO_4 and evaporated under reduced pressure. The residue obtained was purified by silica gel column chromatography (hexane/ethyl acetate, from 100:0 to 95:5) to afford phenol derivative (**iii**) (2.65 g, 42 % yield) that can be crystallized from hexane (mp).

^{1}H NMR (400 MHz, $CDCl_3$) δ 7.49 (s, 1H), 7.26 (d, J = 1.5 Hz, 1H), 3.90 (s, 3H), 3.25 – 3.15 (m, 1H), 2.62 – 2.55 (m, 1H), 2.13 – 1.79 (m, 5H), 1.23 (d, J = 7.0 Hz, 3H), 1.01 (d, J = 6.8 Hz, 3H), 0.84 (d, J = 6.8 Hz, 3H). ^{13}C NMR (100 MHz, $CDCl_3$) δ 168.0, 153.7, 141.5, 135.7, 126.9, 123.3, 113.2, 52.1, 43.1, 33.2, 27.2, 26.8, 21.9, 20.8, 19.4, 19.0. EI-MS *m/z* 262 (24), 231(8), 219 (100), 187 (40), 160 (10), 145 (11), 131 (4), 115 (7), 105 (2), 91 (3); $[\alpha]_D$ (*c* 2, $CHCl_3$): +64.2.

***(+)-8-trans-HC (2)**. (a)* $LiAlH_4$ (300 mg, 7.9 mmol) was added to an ice-bathed, magnetically stirred diethyl ether solution of **(iii)** (1 g, 3.82 mmol). The mixture was stirred for 30 min and then quenched with a saturated aqueous NH_4Cl, acidified with diluted HCl and then extracted with diethyl ether. The combined organic layers were dried over anhydrous Na_2SO_4 and evaporated under reduced pressure.

(b) The crude residue was taken-up with MeOH (25 mL), placed in a round-bottomed flask equipped with a magnetic stirrer and was hydrogenated using 10 % Pd/C (200 mg) as catalyst. The mixture was then filtered and, after evaporating the solvent under reduced pressure, the residue obtained was purified by silica gel column chromatography (hexane:ethyl acetate, from 100:0 to 95:5) to afford (+)-8-*trans*-HC **(2)** (750 mg, 90 % yield).

^{1}H NMR (400 MHz, $CDCl_3$) δ 6.51 (s, 1H), 6.36 (s, 1H), 4.51 (s, 1H), 3.04 – 2.94 (m, 1H), 2.39 (td, J = 5.8, 2.9 Hz, 1H), 2.17 (s, 3H), 1.96 – 1.85 (m, 2H), 1.82 – 1.65 (m, 2H), 1.13 (d, J = 7.0 Hz, 3H), 0.91 (d, J = 6.8 Hz, 3H), 0.75 (d, J = 6.8 Hz, 3H). ^{13}C NMR (100 MHz, $CDCl_3$) δ 168.0, 153.1, 141.1, 135.0, 126.2, 122.9, 113.5, 43.2, 33.1, 27.4, 26.7, 22.0, 21.2, 21.0, 19.6, 19.4. EI-MS *m/z* 218 (29), 203 (2), 175 (100), 160 (13), 147 (12), 141 (4), 128 (4), 121 (5), 115 (6), 105 (2), 91 (4); $[\alpha]_D$ (*c* 2, $CHCl_3$): +29.2.

2.2.2. *TvLac −mediated oxidation of 8-tans-HC: General procedure*

TvLac (0.4U $mg^{-1}_{substrate}$) was added to a 25 mM solution of the selected enantiomer of 8-*trans*-HC prepared in a 50 % v/v mixture of acetone and acetate buffer (50 mM, pH 4.5). The resulting mixture was incubated in orbital shaker at 27 °C under gentle shaking (180 rpm) for 24 h and then extracted with AcOEt. The combined organic layers were dried over anhydrous Na_2SO_4 and evaporated under reduced pressure. The crude residue was purified by silica gel column chromatography using a petroleum ether and AcOEt (95:5) as mobile phase.

*Biooxidation of (−)-8-trans-HC **(1)**.* According to the above described general procedure (2.2.2), the *C*2-C4′ (−)-$(S)_{ax}$-*trans*-HC dimer **1a** (18.6 mg, 0.04 mmol, isolated yield: 25 %, TLC Rf: 0.40) and two mixtures of non-separable C—C (13 mg, 0.03 mmol, isolated yield: 18 %, TLC Rf: 0.60) and C—O dimers (27.0 mg, 0.06 mmol, isolated yield: 38 % TLC Rf: 0.75) were obtained as yellow oils starting from (−)-8-*trans*-HC (70 mg, 0.32 mmol) and *TvLac* (28 U).

1a: ^{1}H NMR (500 MHz, C_6D_6) δ 6.75 (s, 1H), 6.09 (s, 1H), 4.86 (s, 1H), 4.08 (s, 1H), 3.51 (quint. d, J = 7.0, 2.0 Hz, 1H), 3.31 (quint. br, J = 6.9 Hz, 1H), 2.58 (q, J = 4.0 Hz, 1H), 2.50 (td, J = 6.0, 3.0 Hz), 2.06 (m, 1H), 2.05 (m, 1H), 2.03 (m, 1H), 1.96 (m, 2H), 1.96 (m, 1H), 1.91 (m, 1H), 1.90 (s, 3H), 1.87 (s, 3H), 1.74 (m, 1H), 1.50 (m, 1H), 1.41 (m, 1H), 1.38 (d, J = 6.9 Hz, 3H), 1.31 (d, J = 6.9 Hz, 3H), 1.01 (d, J = 6.9 Hz, 3H), 0.88 (d, J = 6.9 Hz, 3H), 0.74 (d, J = 6.9 Hz, 3H), 0.72 (dz, J = 6.9 Hz, 3H). ^{13}C NMR (125 MHz, C_6D_6) δ 153.45, 150.90, 142.21, 139.51, 136.02, 132.20, 128.75, 126.48, 125.58, 123.93, 123.24, 114.86, 22.20, 22.11, 21.71, 21.01, 19.75, 19.72, 19.56, 19.54, 19.49, 18.29.

$[\alpha]_D$ (*c* 1.0, $CHCl_3$): −57.87.

ESI-MS *m/z*: 457.3 $[M + Na]^+$; 473.2 $[M + K]^+$. HRMS (ESI) *m/z* calcd for $C_{30}H_{43}O_2$ $[M + H]^+$: 435.3263, found: 435.3261.

*Biooxidation of (+)-8-trans-HC **(2)**.* According to the above described general procedure (2.2.2), the *C*2-C4′ (+)-$(R)_{ax}$-*trans*-HC dimer **2a** (17.7 mg, 0.04 mmol, isolated yield: 22 %, TLC Rf: 0.37) and two mixtures of non-separable C—C (8.7 mg, 0.02 mmol, isolated yield: 11 %, TLC Rf: 0.44) and C—O dimers (35.6 mg, 0.07 mmol, isolated yield: 39 %) were obtained as yellow oils starting from (+)-8-*trans*-HC (80 mg, 0.37 mmol) and TvLac (28 U).

2a: ^{1}H NMR (400 MHz, $CDCl_3$) δ 6.63 (s, 1H), 6.61 (s, 1H), 4.86 (s, 1H), 4.75 (s, 1H), 4.68 (s, 1H), 3.21–3.10 (m, 2H), 2.49–2.45 (m, 1H), 2.38–2.35 (bt, J = 6 Hz, 1H), 2.05 – 1.99 (m, 3H), 1.85 (s, 3H), 1.82–1.78 (m, 1H), 1.77 (s, 3H), 1.75–1.69 (m, 3H), 1.51–1.45 (m, 2H), 1.19 (d, J = 6.9 Hz, 3H), 1.10 (d, J = 6.9 Hz, 3H), 0.98 (d, J = 6.9 Hz, 3H), 0.85 (d, J = 6.9 Hz, 3H), 0.64 (d, J = 6.9 Hz, 3H), 0.61 (d, J = 6.9

Hz, 3H). ^{13}C NMR (101 MHz, $CDCl_3$) δ 152.9, 150.3, 142.3, 139.3, 136.3, 131.9, 128.3, 126.1, 125.9, 123.5, 122.9, 114.6, 43.1, 39.6, 33.1, 31.9, 27.2, 26.9, 26.6, 26.6, 22.1, 22.1, 21.6, 20.7, 19.8, 19.6, 19.5, 19.5, 17.8.

$[\alpha]_D$ (*c* 1.5, $CHCl_3$): +48.0.

ESI-MS *m/z*: 457.3 $[M + Na]^+$; 473.2 $[M + K]^+$. HRMS (ESI) *m/z* calcd for $C_{30}H_{43}O_2$ $[M + H]^+$: 435.3263, found: 435.3262.

2.3. Computational chemistry

2.3.1. Molecular dynamics

All molecular dynamics (MD) simulations either without or with the enhanced-sampling algorithms provided by Plumed [53] and all the standard structural analyses were performed with AMBER 23 suite [54,55] with the CUDA implementation for GPUs. The molecules reported in Fig. 5 (*i.e.* the two axial diastereoisomers of dimers **1a** and **2a**) and methanol were parametrized using the webserver https://www.charmm-gui.org using charmm36 force field [56–58]. In the same webserver was possible to set up the systems for the MD simulations by placing the solute dimer in a cubic box with volume of 125 nm^3, the box was then filled by methanol molecules until reach the right density of 0.79 g/cm^3. Each system before the production MD simulation were minimized for 5000 steps with steep-descent algorithm. The minimized systems were then equilibrated at 300 K for 5000 ps using Langevin coupling, with γ equal to 1 ps^{-1} and a non-bonded cut-off of a 12 A with an integration step of 0.001 ps. The NPT production MD was run at 300 K for $50*10^3$ps using Langevin coupling, with γ equal to 1 ps^{-1} and non-bonded cut-off of a 12 A with MC barostat with an integration step of 0.002 ps [59]. Trajectory frames for subsequent analysis were saved every 5 ps for a total of 10,000 conformations. The conformational space of the two unsaturated 6-membered rings, menthol moieties, was sampled more extensively using metadynamics with the puckering collective variable described by Cremer and Pople in 1975 and implemented in Plumed as collective variable (CV) by Parrinello and colleagues in 2007 (plumed version 2.8.1) [60,61]. The enhanced sampling was applied by adding a hill in cartesian coordinates every 250 steps with a width of 0.05 and height of 0.05 $kj*mol^{-1}$. To speed up the convergence of the simulations, the BIASFACTOR parameter was set equal to 20. Plumed energetic log (colvar, hills) files were saved every 250 steps, the data used for the clustering analysis were generated by recalculating the CV on every frame keep during the MD. The collective variable is written in two forms inside the Plumed log files: one in spherical coordinates (ϕ, ψ, ρ) and in its projection on the Cartesian axis (X,Y,Z).

2.3.2. Clustering

The projection of the collective variable on the 3 Cartesian axes was analysed by clustering analysis in order to determine the most probable conformations sampled by the two molecules during the MD simulations. The R-cuda implementation of the kmeans algorithm was used for clustering analysis and a total of 30 unique conformations were identified for each molecule [62,63]. The clustering algorithm was first applied on the CV in cartesian coordinated of one ring and the clusters were identified. Then all conformations belonging to a cluster were further clustered by considering the CVs in Cartesian coordinates of the second ring.

2.3.3. Electronic circular dichroism (ECD) spectra calculation

The QM calculations were repeated on each of the 30 unique conformations identified by the clustering analysis for the molecules reported in Fig. 3, *i.e.* the two axial diastereoisomers of dimers **1a** and **2a**. The ECD spectra were calculated with Gaussian v.16 at DFT/TDDFT level using for all the calculation the functional PBE1PBE with the basis set 6–311 + G**. [64–66]. The solvation model used to mimic the effect of methanol on the molecule is Polarizable Continuum Mode (PCM) with permittivity ε = 32.613F/m [https://doi.org/10.1021/cr9904009] [67]. All conformations found by clustering analysis were minimised and the minimum conformations were verified to be true minima by frequency calculation. From frequency calculation were also saved the free energies and the zero-point energy (ZPE) that will be used later for the mean ECD spectra calculation. With the TDDFT were calculated the ECD spectra and were calculated the first 60 singlet excited states. Using the program SpecDis version 1.71 was possible analyse and calculate the ECD mean spectra. [68,69] The Boltzmann-weighted summation was used to calculate the mean ECD spectra using the free energy corrected by the ZPE.

2.3.4. Rotational energy barrier estimation

Metadynamics was used to sample the probable conformations adopted by molecule dimer **2a** during the rotation around the bond that generate atropisomerism, *i.e. T1* [67]. The MD protocol is the same described in section 2.3.1 but the collective variable this time is the torsion *T1* and the enhanced sampling was applied by adding a hill in cartesian coordinates every 250 steps with a width of 0.15 and height of 0.15 $kj*mol^{-1}$. The clustering analysis on 10,000 conformations, as described in section 2.3.2, for T1 select 17 conformations. The energies of these conformation were evaluated by DFT using for all the calculation the functional B3LYP with the basis set 6-31G.

2.4. Biology

2.4.1. Promastigote stage of Leishmania spp cultures and antileishmanial activity

Promastigote stage of *L. infantum* strain (MHOM/TN/80/IPT1, kindly provided by Dr. M. Gramiccia and Dr. T. Di Muccio, ISS, Roma) and *L. tropica* (MHOM/IT/2012/ISS3130) were cultured in RPMI 1640 medium (EuroClone) supplemented with 15 % heat-inactivated fetal calf serum (EuroClone), 20 mM Hepes, and 2 mM L-glutamine at 22 °C. The MTT (3-[4.5-dimethylthiazol-2-yl]-2.5-diphenyltetrazolium bromide) method [11,14] was used to estimate the 50 % inhibitory concentration (IC_{50}), with some modifications. Compounds were dissolved in DMSO and then diluted with medium to achieve the required concentrations. Drugs were placed in 96 wells round bottom microplates and seven serial dilutions made. Amphotericin B was used as the reference antileishmanial drug. Parasites were diluted in complete medium to 5 x 10^6 parasites/mL and 100 µl of the suspension was seeded into the plates, incubated at 22 °C for 72 h. Then 20 µl of MTT solution (5 mg/mL) was added into each well, after 3 h the plates were centrifuged, the supernatants discarded and the resulting pellets dissolved in 100 µl of lysing buffer consisting of 20 % (w/v) of a solution of SDS (Sigma), 40 % of N, *N*-dimethylformamide (Merck) in H_2O. The absorbance of the obtained solutions was measured at a wavelength of 550 nm with a reference at 650 nm with a microplate spectrophotometer (Synergy 4-Biotek) and analyzed with the Gen5® software for data processing. The results are expressed as IC_{50}, the dose of compound is necessary to inhibit cell growth by 50 %; each IC_{50} value is the mean ± standard deviation of at least three separate experiments performed in duplicate [11,14].

2.4.2. P. Falciparum cultures and drug susceptibility assay

P.f. cultures were carried out according to Trager and Jensen with slight modifications [70]. The CQ-susceptible strains D10 and the CQ-resistant strain W2 were maintained at 5 % hematocrit (human type A-positive red blood cells) in RPMI 1640 (EuroClone, Celbio) medium with the addition of 1 % AlbuMax (Invitrogen, Milan, Italy), 0.01 % hypoxanthine, 20 mM Hepes, and 2 mM glutamine. All the cultures were maintained at 37 °C in a standard gas mixture (1 % O_2,5%CO_2, and 94 % N_2). All compounds were dissolved in either water or DMSO and then diluted with medium to achieve the required concentrations (final DMSO concentration < 1 %, non-toxic to the parasite). Drugs were placed in 96-well flat-bottomed microplates (Costar) and serial dilutions made. Asynchronous cultures with parasitaemia of 1–1.5 % and 1 % final hematocrit were aliquoted into the plates and incubated for 72 h at

37 °C. Parasite growth was determined spectrophotometrically (OD650) by measuring the activity of the parasite lactate dehydrogenase (pLDH), according to a modified version of the method of Makler in control and drug-treated cultures. The antiplasmodial activity is expressed as 50 % inhibitory concentrations (IC_{50}); each IC_{50} value is the mean ± standard deviation of at least three separate experiments performed in duplicate [15,16].

2.4.3. Cytotoxicity against HepG2 cell line

HepG2 is a cell line exhibiting epithelial-like morphology that was isolated from a human hepatocellular carcinoma. Cells were maintained in standard conditions at 37 °C in 5 % CO_2 incubator in DMEM medium, supplemented with 10 % fetal calf serum and 2 mM glutamine. For the toxicity experiments, HepG2 cells at 1.5 x 10^4 cells/100 µl/well were plated in 96-well plates and incubated at 37 °C, 5 % CO_2 overnight. Cells were than treated with serial dilutions of test compounds for 72 h, and cell proliferation was evaluated by using the MTT assay already described [71].

3. Results & discussion

3.1. A novel chemo-enzymatic synthesis of bicalamenenes

The preparation of (−)-*trans*-HC was previously accomplished starting from (−)-menthol applying a synthetic protocol developed by us [47]. Accordingly, (+)-8-*trans*-HC was synthesized in the framework of this study *via* the straightforward application of the same synthetic strategy but using the commercially available (+)-menthol as starting material (Scheme 2).

Briefly, (+)-menthol was oxidized to the corresponding ketone (**i**) that underwent a two-step process of carbon homologation based on the Shapiro reaction to afford the aldehyde (**ii**). This compound was converted into the bicyclic phenol (**iii**) *via* C4 homologation to the corresponding substituted 3,5-hexadienoic acid followed by a benzannulation reaction [48]. Finally, target (+)-*trans*-HC was obtained *via* two sequential reduction steps. Accordingly, compound (**iii**) was treated with $LiAlH_4$ that reduced the benzoic ester group into the corresponding benzylic alcohol group. The intermediate was not isolated and was further reduced to (+)-*trans*-HC by hydrogenation in the presence of Pd/C as catalyst [47].

The core of the proposed chemo-enzymatic bicalamenene synthesis was the biocatalyzed oxidative dimerization of the above described 8-*trans*-HC mediated by the laccase from *T. versicolor* (*TvLac*). *TvLac* catalysis allows, in fact, the activation of normally inert Csp^2-H bonds (generally of phenols and anilines) as highly reactive radical species under mild conditions, at the only expense of molecular oxygen and forming water as the byproduct of the process. The destiny of the formed radical(s) can vary from simple functional group oxidation, C—H hydroxylation and C—C or C—O dimerization, to the production of complex carbonaceous skeletons *via* multistep mechanisms relaying on the chemical features of the substrates [49,50]. We previously reported the exploitation of this enzymatically triggered radical-cation chemistry to, *e.g.*, successfully prepare heterocyclic derivatives of naturally occurring phenols. In this way benzofuran-based libraries of antioxidant NPs and of allosteric ligands of the molecular chaperone Hsp90 were obtained [13,72–74]. Moreover, this approach allowed us to easily prepare C—C dimers of phenolic NP and, most importantly in the context of this work, to install stereogenic axes on the obtained dimeric products [51,75].

Thrilled by these findings and aiming at synthesizing bicalamenenes, we investigated the reaction outcomes of the biooxidation of (−)-8-*trans*-HC (**1**, selected as model substrate) catalyzed by *TvLac*. Briefly, the biotransformation was first investigated on analytic scales to identify the proper reaction medium, evaluating the substrate conversion and the product(s) formation by simple TLC analyses. Different water miscible cosolvents (methanol, acetonitrile, acetone, dimethyl sulfoxide and dimethyl formamide) were investigated using different v/v ratios working in the presence of increasing substrate and enzyme loadings (1–10 $mg_{substrate}$ mL^{-1} and U $mg^{-1}_{substrate}$, respectively), and selecting acetate buffer (50 mM, pH 4.5) as the main reaction solvent. Biphasic systems (50 % v/v of AcOEt) were also considered. Eventually, balancing different factors, a 25 mM solution of (−)-8-*trans*-HC prepared in a 50 % v/v solution of acetone in acetate buffer in the presence of *TvLac* (0.4 U $mg^{-1}_{substrate}$) was selected to proceed with the preparative scale reactions. Specifically, we considered (1) substrate's solubility, (2) the enzyme stability (measured as residual activity following reported protocols [51]), (3) substrate's conversion and (4) the formation of TLC spots characterized by retention factors (Rf) potentially attesting for unitary dimers instead of oligomers/degradation products.

Accordingly, (−)-8-*trans*-HC was oxidized with *TvLac* and the obtained mixture was purified *via* flash column chromatography on silica gel isolating in both cases the products corresponding to three different TLC spots having the following Rf (petroleum ether/AcEOt = 95:5): 0.75, 0.60 and 0.35 (Scheme 3a).

Products were at first characterized by ESI-MS and ^{1}H NMR. While all the three products shared a mass value compatible with dimeric structures of (−)-8-*trans*-HC, only the most polar spot (dimer **1a**, Rf: 0.35) was identified to be a single product. On the contrary, the other two isolated materials, corresponding to the TLC spots with Rf 0.75 and 0.60, revealed themselves as inseparable and not-fully characterizable mixtures of dimers, with the former potentially being an ensemble of different regioisomeric C—O dimers according to the lower polarity. The structure of **1a** was elucidated by NMR (Table S1 of SI) on the basis of NOE experiments recorded in C_6D_6 (Scheme 3b).

According to the structure reported in Scheme 3 the proton H-4

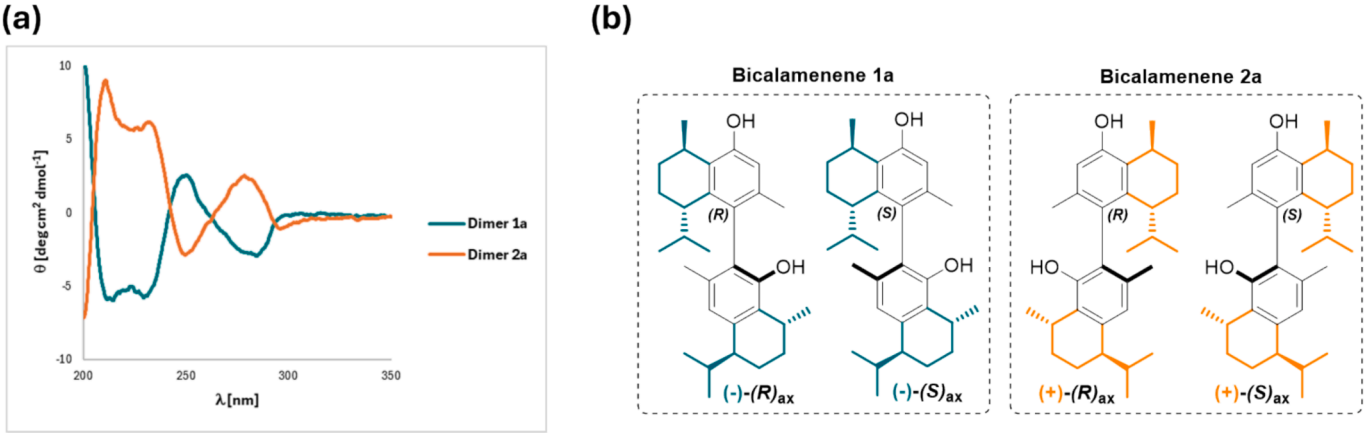

Fig. 3. (a) Experimental EDC spectra of dimer **1a** and dimer **2a**. (b) Structures of the four stereoisomeric bicalamenene applied in the DFT calculations.

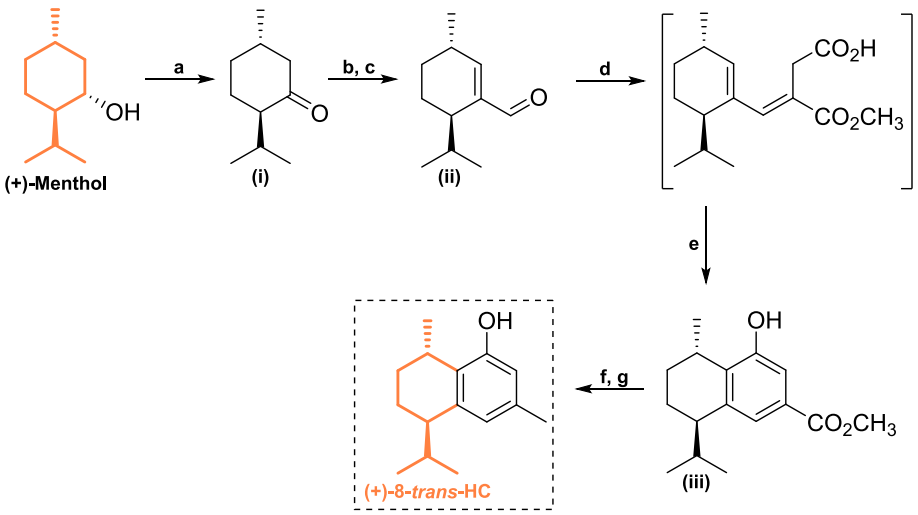

Scheme 2. Chemical synthesis of (+)-8-*trans*-HC. Reagents and conditions: *(a)* Jones reagent, diethyl ether, ice bath; *(b)* *p*-toluenesulfonyl hydrazine, DCM, 0 °C; *(c)* 2:1 mixture of hexane/TMEDA, BuLi, DMF, from −78 °C to 24 °C; *(d)* LDA, dimethyl succinate, THF, from −60 °C to 24 °C; *(e)* TEA, trifluoroacetic anhydride, THF, 24 °C; *(f)* $LiAlH_4$, diethyl ether, 0 °C; *(g)* 10 % Pd/C,H_2 gas, MeOH, 24 °C.

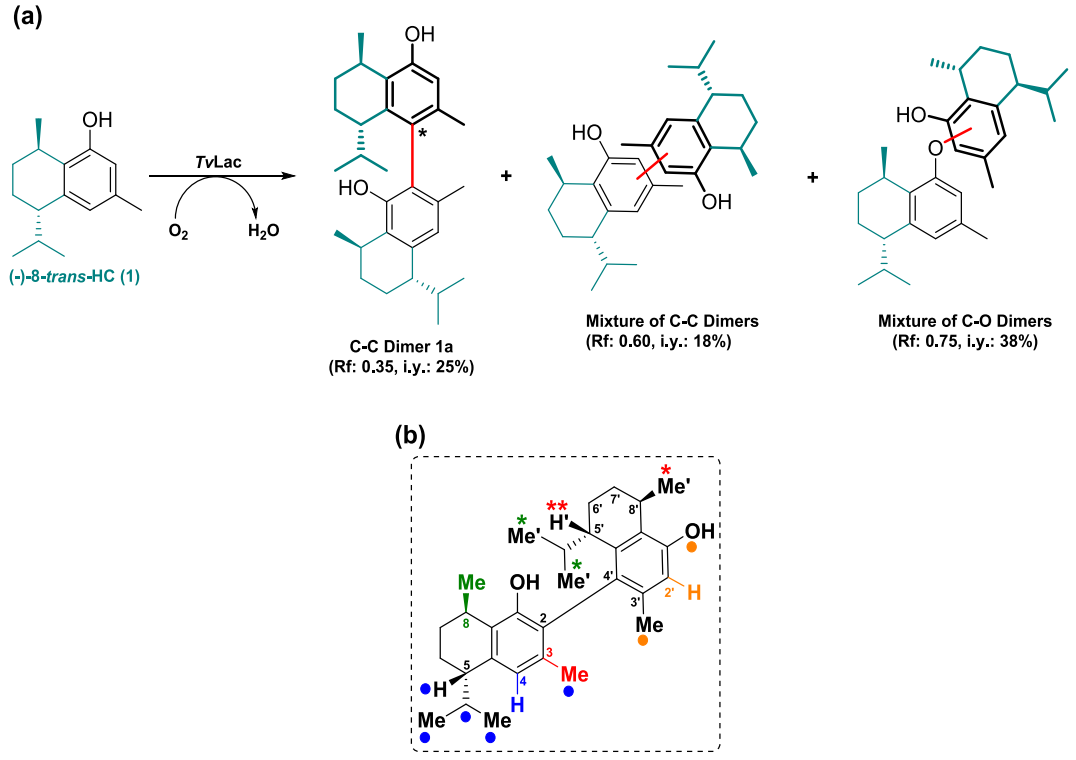

Scheme 3. **(a)** *TvLac*-mediated oxidation of (−)-8-*trans*-HC and the corresponding isolated products. (**b**) Schematization of the NOE effects related to the to the H-4 and H-2′ nuclei (●, depicted respectively in blue and orange) and to the Me-3 and Me-8 groups (*, depicted respectively in red and green) of dimer **1a**.

shows NOEs with the Me-3, H-5 and the C5-isopropyl group while H-2′ displays effects only with Me-3′ and OH-1′ thus confirming that the dimerization occurred between the C-2 and C-4′ carbons.

As specified by different literature reports [32,33,40,45,46], bicalamenenes exist as stable atropisomers, stereoisomers formed when the energy differences due to steric strain (or other contributors) create on a single C—C bond a rotational barrier high enough to allow the isolation of the individual conformers. In the case of the bicalamenene **1a**, the conformational freedom of the Csp^2-Csp^2 single bond connecting the two calamenene units is potentially limited by the steric interaction of the methyl, hydroxy and isopropyl groups close to carbons *C*2 and C4′.

Considering that the thermal energy of a free molecule in solution is estimated to be 25 kcal mol^{-1}, we proceeded to calculate the barrier rotational energy of the *C*2-C4′ single bond *via* Density Functional Theory (DFT). An energy barrier of 28.40 kcal mol^{-1} was obtained, suggesting the presence of a conformationally restricted diaryl system and the establishment of a stereogenic axis stable at room temperature. Accordingly, some NOEs observed between nuclei belonging to the two

calamenene units further advised for a rigid spatial orientation of the two terpene units along the *C*2-C4′ axis and allowed also to hypothesise their relative orientation in the space. In particular, the methyl Me-3 (1.90 ppm) showed strong contacts with H-5′ (2.58 ppm) and weaker NOE effects with Me-8′ (1.31 ppm) and the methyl Me-8 (1.38 ppm) weakly interacted with the Me' (isop) (0.72 ppm). These observations could imply that the substituted cyclohexene ring of **1a** (carbons C-5′, C-6′, C-7′, C-8′) should be oriented at the same side of the Me-8 methyl group (Scheme 3b). Moreover, the NMR spectra of dimer **1a** suggested that the biooxidation resulted in the formation of only one atropoisomeric bicalamenene, as single sets of signals were registered attesting the presence of only one of the two possible diastereomeric dimers (Fig. 3b).

The laccase mediated oxidation of (+)-*trans*-8-HC, conducted in the same optimized conditions used for the (−)-enantiomer, gave very similar results (Scheme 4). The characterization of dimer **2a** can be found in the SI and agrees with the structural data reported by Nishizawa *et al.* in 1985 for a naturally occurring bicalamenene synthetically derived from (+)-8-*trans*-HC [40].

3.2. Determination of the absolute configuration of dimers *1a* and *2a*

The next step of our investigation was the elucidation of the stereochemical outcome of the biooxidation reactions. The optical rotatory power (α_D) of **1a** and **2a** were measured and the two bicalamenenes shared their steric series with their respective parental compounds as a positive value was obtained for the former and a negative one for the latter. Electronic circular dichroism (EDC) analyses were than conducted on **1a** and **2a** to investigate the stereochemical relationship of the two compounds which could be atropoenantiomers or atropodiastereomers, depending on the absolute configuration of their stereogenic axes. Obtained EDC spectra (Fig. 3a) attested that the two biscalamenenes are enantiomers in nature suggesting that the *TvLac*-mediated oxidative coupling of their parental compounds occurred *via* a stereospecific mechanism. Similar results were reported in 1985 for the $FeCl_3$-triggered dimerization of (+)-8-*trans*-HC as only one atropisomer, characterized by the same connectivity of dimer **2a**, was obtained from the enantiopure substrate [40]. The identical ^{1}H NMR spectra of **1a** and **2a** (see the $CDCl_3$ spectra reported in the SI) further confirmed their atropoenantiomeric stereochemical relationship highlighting that the two dimers are the two enantiomeric forms of the same bicalamenene.

To assign the absolute configuration of the stereogenic axes installed on the couple of enantiomeric dimers **1a** and **2a**, a strategy based on the *in-silico* prediction of the experimentally EDC spectra of the two isolated atropisomers was applied. Briefly, the ECD spectra of the four possible diastereoisomers that could theoretically be obtained from the biooxidation of the enantiomers of 8-*trans*-HC (Fig. 3b) were simulated *via* DFT calculations and compared to experimentally obtained ones, according to literature protocols applied to similar cases [69,76,77].

Although the four molecules appear to lack significant degrees of freedom around the stereogenic axes that generates the atropisomerism, the two terpene (*p*-menthane) moieties may retain some conformational freedom. Accordingly, to properly describe the conformational dynamics of the two dimers in solution, metadynamics simulations were used, since they allow to sample the conformational space with greater efficiency in less time than normal molecular dynamics (MD) [60,61]. Obtained results confirmed the initial hypothesis and highlighted that the *p*-menthane moieties occupy a wide range of conformations, as depicted by the tight blue cloud of Fig. 4, with some exhibiting greater stability than the others and thus sampled during the simulations. The dynamicity of the *p*-menthanes were described in this way by 30 stable (and unique) conformations that were this used for the calculation of dimers **1a** and **2a** ECD spectra (Fig. 5). For more details consult the Supporting information Fig. S1, which summarized the significant fluctuations in the collective variable in Cartesian coordinates and Table S2 in which the clustering analysis of the conformations sampled during the metadynamics simulations is reported.

All the 30 conformations for each dimer were first minimized at quantum mechanical level using DFT with 6-311G** as basis set. The subsequent frequency analysis was used to verify that all the final conformations were all local minimum, their heat of formation, corrected by the zero-point energy (ZPE), are reported in Table S2 of the SI. The program SpectDis v1.71 was used to analyze and visualize the ECD spectra calculated with Gaussian [66,68,69]. The final spectrum for each of the four stereoisomeric dimers (reported and compared with the experimental ones in Fig. 5) was the result of the Boltzmann weighted sum over all 30 conformations representing its conformational freedom.

Furthermore, the program enabled the calculation of the degree of similarity (reported as Similarity Indexes in Fig. 5) between the experimental ECD spectra of **1a** and **2a** and the simulated spectra of the corresponding axial atropoisomeric diastereoisomers (*i.e.* (−)-$(R)_{ax}$ or (−)-$(S)_{ax}$ bicalamenene and (+)-$(R)_{ax}$ or (+)-$(S)_{ax}$ bicalamenene, respectively). Besides simple qualitative confrontations, these indexes were therefore employed to assign the absolute conformation of dimers **1a** and **2a**. Accordingly, dimer **1a** was identified as the (−)-$(S)_{ax}$ stereoisomer (Similarity Index = 0.8511), while compound **2a**, as expected, was associated with the absolute configuration of its enantiomer, the (+)-$(R)_{ax}$ stereoisomer (Similarity Index = 0.7279).

Based on the NOE effects described in the previous paragraph, it was hypothesized that the carbonaceous skeleton of the substituted cyclohexene ring of one *p*-menthane moiety (carbons C-5′, C-6′, C-7′, C-8′) and the Me-8 group of the other one should be oriented in the same way with the respect to the stereogenic axis of **1a**. Similarly, the Me-3 group of one calamenene unit should be spatially near to the H'-5 on the other *p*-menthane moiety. A snapshot of MD simulation of the (−)-$(S)_{ax}$ enantiomer of dimer **1a** demonstrated that its DFT-attributed absolute

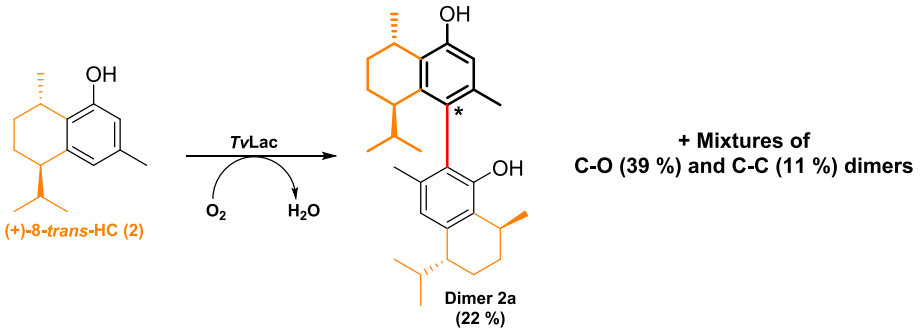

Scheme 4. *TvLac* mediated oxidation of (+)-8-*trans*-HC.

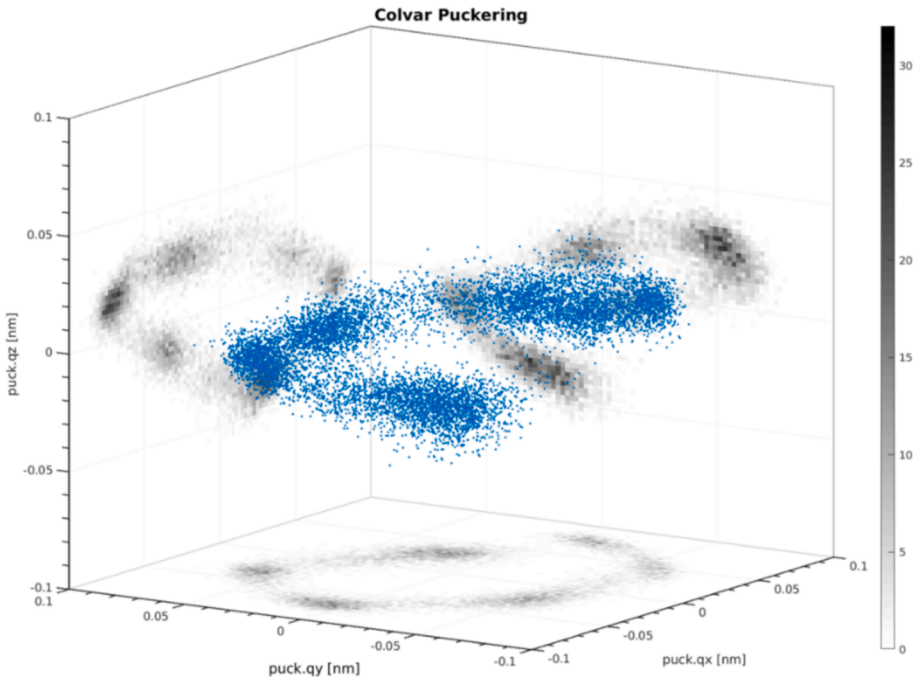

Fig. 4. Each blue point represents a conformation sampled during the MD simulation for one of the *p*-menthane moieties in Cremer and Pople puckering coordinates. The points were projected onto the three Cartesian planes (xy,xz,yz), with darker colors indicating a greater concentration of conformations in that area as shown by the gray scale of the color bar. (For interpretation of the references to color in this figure legend, the reader is referred to the web version of this article.)

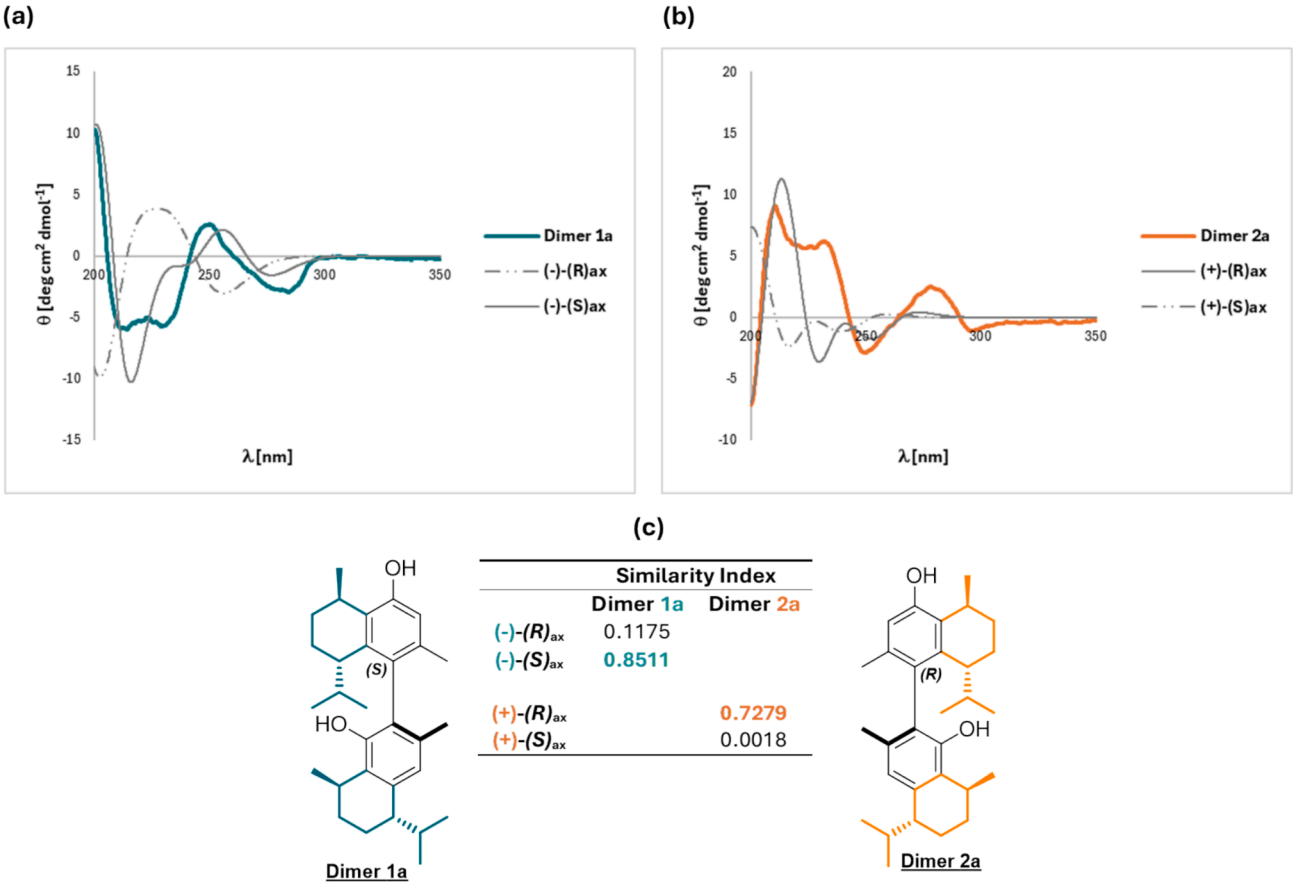

Fig. 5. Experimental EDC spectra of dimer **1a (a)** and of dimer **2a (b)** confronted with the simulated EDC spectra of their corresponding diastereoisomeric atropisomers. **(c)** Similarity indexes between the experimental and the simulated ECD spectra and the identified absolute configurations of **1a** and **2a**.

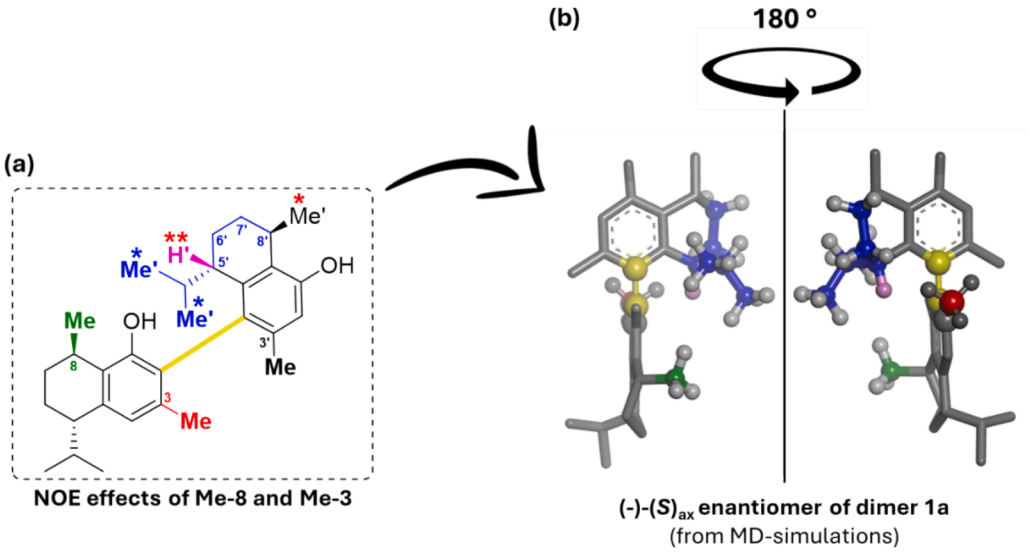

Fig. 6. Schematization of the NOE effects involving the Me-3 and Me-8 groups (*) of dimer **1a** and two different views of one of its MD-simulated (−)-$(S)_{ax}$-configured conformers. The stereogenic axis is depicted in yellow, while Me-8, Me-3, hydrogen H-'5 and carbons C-5′, C-6′, C-7′, C-8′ respectively in green, red, pink and blue. (For interpretation of the references to color in this figure legend, the reader is referred to the web version of this article.)

configuration agreed with the NMR-suggested spatial orientation of the Me-8 and Me-3 groups (Fig. 6). Accordingly, the Me-8 group (green coloured) and carbons C-5′, C-6′, C-7′, C-8′ (blue coloured) were properly placed on the same side of the stereogenic axis (depicted in yellow) as well as the Me-8 group (red coloured) and the H'-5 hydrogen atom (pink coloured).

3.3. Antiprotozoal activity profiling

The two parental enantiomers of 8-*trans*-HC and their corresponding atropoisomeric C—C dimers were subjected to an *in vitro* campaign to profile, for the first time, their antiprotozoal activity *via* phenotypic screenings. Specifically, their growth inhibitory activity was assessed against cultures of *P.f.* parasites and against promastigotes of *Leishmania infantum* and *Leishmania tropica*. Also, compounds' cytotoxicity was preliminarily assessed against the human cell line HepG2. Obtained results are summarized in Table 1.

In general, the parental calamenenes demonstrated a high-micromolar range growth inhibitory activity against both the selected human cell lines and the parasites culture. Specifically, the compounds showed a very modest leishmanicidal activity while their potency was slightly higher against *P.f.* cultures. Moreover, compounds were active against both the chloroquine (CQ)-sensitive DC10 and the CQ-resistant W2 *P.f.* strains. Regardless this, both were poorly selective, as assed by their calculated selectivity index (S.I.).

The two dimers (compounds **1a** and **2a**) showed a modest decrease in their aspecific cytotoxicity with the respect to both the parental compounds. Only in the case of the (+)–HC dimer (**2a**), a more potent leishmanicidal activity, even if this still in the high-micromolar range, was attested while the (−)–HC dimer (**1a**) resulted less active than its parental compound (−)-8-*trans*-HC (**1**).

Interestingly, both the dimers were associated with an increase in their antiplasmodial activity. Specifically, the (−)–HC dimer (**1a**) and the (+)–HC dimer (**2a**) were found to be 10 and 20-times more potent than the corresponding 8-*trans*-HCs against the resistant W2 *Pf* strain, respectively. According to the collected data, their calculated S.I. were also improved. Moreover, both the dimers, as their corresponding parental compounds, did not demonstrate any sign of cross-resistance (resistance indexes (R.I.) $\leq$ 1).

4. Conclusions

A novel and reliable chemo-enzymatic synthesis of the atropoisomeric dimers 8-*trans*-hydroxycalamenene (*i.e.* the corresponding *C*2-C4′ bicalamenenes) was successfully validated starting from commercially available (−)- and (+)-menthol. Specifically, the core of the proposed synthetic entry was a biooxidation of 8-*trans*-hydroxy calamenene mediated by the laccase from *Trametes versicolor* which resulted in the stereospecific preparation of the (−)-*trans-(S)*$_{ax}$ *C*2-C4′ bicalamenene and the (+)-*trans-(R)*$_{ax}$ *C*2-C4′ bicalamenene starting, respectively, from

Table 1
Phenotypic screening for antiprotozoal activity against *Leishmania* spp and *P.f.* parasites cultures.

Growth Inhibitory Activity IC_{50} (μM)							
	Plasmodium falciparum				*Leishmania* spp Promastigotes		*Human cell line*
	D10 strain[1]	W2 strain[2]	S.I.[3]	R.I.[4]	*L. infantum*	*L. tropica*	HepG2[5]
(−)-8-*trans*-HC (1)	24.5 ± 7.0	13.1 ± 1.6	5	< 1	51.8 ± 1.4	36.4 ± 8.1	70.0 ± 9.3
(−)-Dimer (1a)	2.7 ± 0.5	1.3 ± 0.1	23	< 1	> 45	> 45	29.5 ± 7.0
(+)-8-*trans*-HC (2)	28.1 ± 9.9	27.0 ± 10.0	2	1	58.5 0 ± 0.6	80.7 ± 7.1	56.3 ± 6.4
(+)-Dimer (2a)	3.2 ± 0.6	1.3 ± 0.2	24	< 1	34.6 ± 0.1	23.4 ± 1.6	30. 8 ± 6.6
CQ[6]	0.023 ± 0.006	0.5 ± 0.1	22	80	N.T.[8]	N.T.[8]	40.0 ± 9.5
Amph B[7]	N.T.[8]	N.T.[8]	N.D.[9]	N.D.[9]	0.160 ± 0.005	0.150 ± 0.005	59.1 ± 10.6

[1] Chloroquine-sensitive *P.f.* strain; [2] Chloroquine-resistant *P.f.* strain; [3] Selectivity Index (SI): $IC_{50}^{HepG2}/IC_{50}^{P.f.\ W2}$ strain; [4] Resistant Index (RI): $IC_{50}^{W2}/IC_{50}^{D10}$; [5] Immortalized cell line derived from liver cancer cell line; [6] CQ = chloroquine, reference antiplasmodial drug; [7] Amph B = amphotericin B, reference leishmanicidal drug; [8] Not tested; [9] Not defined.

the (−)- and the (+)-enantiomer of the aforementioned terpene.

The connectivity and the absolute configuration of the obtained *C*2-C4′ bicalamenene was defined *via* an integrated strategy comprising 2D-NMR spectroscopy, electronic circular dichroism and DTF calculations.

Moreover, both the parental terpenes and the obtained bicalamenene were screened *in vitro* for their leishmanicidal and antiplasmodial activity, profiling, for the first time, their potentialities as antiprotozoal agents as purified molecules. Interestingly, both the bicalamenenes were found to be significantly more active than the corresponding calamenene against a drug-resistant *P. falciparum* strain (IC_{50} in the micromolar range) further highlighting the potentialities of building dimers adducts of bioactive natural products to enhance their pharmacological properties [41–44].

Even if none of the screened natural occurring compounds showed antiprotozoal potencies comparable to the hit compounds previously reported by us [11,14–16], this work paves the way to the development of novel potential antiplasmodial agents starting from the skeleton of this peculiar atropoisomeric terpenoids and to perform *ad hoc* designed interactome studies [78,79].

CRediT authorship contribution statement

Ivan Bassanini: Writing – review & editing, Writing – original draft, Validation, Supervision, Project administration, Methodology, Investigation, Formal analysis, Data curation, Conceptualization. **Chiara Tognoli:** Writing – review & editing, Investigation, Data curation. **Massimiliano Meli:** Software, Investigation, Data curation. **Silvia Parapini:** Methodology, Investigation, Formal analysis. **Nicoletta Basilico:** Methodology, Investigation. **Giovanni Fronza:** Investigation, Formal analysis, Data curation. **Stefano Serra:** Validation, Formal analysis, Data curation. **Sergio Riva:** Validation, Supervision, Formal analysis, Conceptualization.

Funding

Financial support from the National Recovery and Resilience Plan (NRRP), Mission 4 Component 2 Investment 1.4 – Call for tender No. 3138 of 16 December 2021, rectified by Decree n. 3175 of 18 December 2021 of Italian Ministry of University and Research funded by the European Union – NextGenerationEU. Project code CN_00000033, Concession Decree No. 1034 of 17 June 2022 adopted by the Italian Ministry of University and Research, CUPB83C2200293006, Project title "National Biodiversity Future Center – NBFC" is kindly acknowledged.

Declaration of competing interest

The authors declare that they have no known competing financial interests or personal relationships that could have appeared to influence the work reported in this paper.

Acknowledgement

We acknowledge the CINECA award under the ISCRA initiative, for the availability of high-performance computing resources and support.

Appendix A. Supplementary data

Supplementary data to this article can be found online at https://doi.org/10.1016/j.bioorg.2024.107917.

Data availability

Data will be made available on request.

References

[1] F. Chappuis, S. Sundar, A. Hailu, H. Ghalib, S. Rijal, R.W. Peeling, J. Alvar, M. Boelaert, Visceral leishmaniasis: What are the needs for diagnosis, treatment and control? Nat. Rev. Microbiol. 5 (2007) 873–882, https://doi.org/10.1038/nrmicro1748.
[2] R.T. Gazzinelli, P. Kalantari, K.A. Fitzgerald, D.T. Golenbock, Innate sensing of malaria parasites, Nat. Rev. Immunol. 14 (2014) 744–757, https://doi.org/10.1038/nri3742.
[3] World Health Organization, Leishmaniasis, (2023). https://www.who.int/news-room/fact-sheets/detail/leishmaniasis (accessed December 12, 2023).
[4] World Health Organization, World Malaria Report, 2023. https://www.who.int/publications/i/item/9789240086173 (accessed December 12, 2023).
[5] R. Capela, R. Moreira, F. Lopes, An Overview of Drug Resistance in Protozoal Diseases, Int. J. Mol. Sci. 20 (2019) 5748, https://doi.org/10.3390/IJMS20225748.
[6] E.G. Tse, M. Korsik, M.H. Todd, The past, present and future of anti-malarial medicines, Malaria Journal 2019 18:1 18 (2019) 1–21. 10.1186/S12936-019-2724-Z.
[7] S. Sundar, J. Chakravarty, Leishmaniasis: an update of current pharmacotherapy, Expert Opin. Pharmacother. 14 (2013) 53–63, https://doi.org/10.1517/14656566.2013.755515.
[8] E.Y. Klein, Antimalarial drug resistance: A review of the biology and strategies to delay emergence and spread, Int. J. Antimicrob. Agents 41 (2013) 311–317, https://doi.org/10.1016/j.ijantimicag.2012.12.007.
[9] L. Cui, S. Mharakurwa, D. Ndiaye, P.K. Rathod, P.J. Rosenthal, Antimalarial drug resistance: Literature review and activities and findings of the ICEMR network, Am. J. Trop. Med. Hyg. 93 (2015) 57–68, https://doi.org/10.4269/ajtmh.15-0007.
[10] A.M. Dondorp, P. Ringwald, Artemisinin resistance is a clear and present danger, Trends Parasitol. 29 (2013) 359–360, https://doi.org/10.1016/j.pt.2013.05.005.
[11] I. Bassanini, S. Parapini, N. Basilico, A. Sparatore, Novel hydrophilic riminophenazines as potent antiprotozoal agents, ChemMedChem 14 (2019) 1940–1949, https://doi.org/10.1002/cmdc.201900522.
[12] A. Koval, I. Bassanini, J. Xu, M. Tonelli, V. Boido, F. Sparatore, F. Amant, D. Annibali, E. Leucci, A. Sparatore, V.L. Katanaev, Optimization of the clofazimine structure leads to a highly water-soluble C3-aminopyridinyl riminophenazine endowed with improved anti-Wnt and anti-cancer activity in vitro and in vivo, Eur. J. Med. Chem. 222 (2021) 113562, https://doi.org/10.1016/J.EJMECH.2021.113562.
[13] I. Bassanini, I. D'Annessa, M. Costa, D. Monti, G. Colombo, S. Riva, Chemoenzymatic synthesis of (E)-2,3-diaryl-5-styryl- trans -2,3-dihydrobenzofuran-based scaffolds and their in vitro and in silico evaluation as a novel sub-family of potential allosteric modulators of the 90 kDa heat shock protein (Hsp90), Org. Biomol. Chem. 16 (2018) 3741–3753, https://doi.org/10.1039/c8ob00644j.
[14] I. Bassanini, S. Parapini, E.E. Ferrandi, E. Gabriele, N. Basilico, D. Taramelli, A. Sparatore, Design, synthesis and in vitro investigation of novel basic celastrol carboxamides as bio-inspired leishmanicidal agents endowed with inhibitory activity against leishmania Hsp90, Biomolecules 11 (2021) 56, https://doi.org/10.3390/biom11010056.
[15] I. Bassanini, S. Parapini, N. Basilico, D. Taramelli, S. Romeo, From DC18 to MR07: a metabolically Stable 4,4′-oxybisbenzoyl amide as a low-nanomolar growth inhibitor of p. falciparum, ChemMedChem 17 (2022) e202200355, https://doi.org/10.1002/CMDC.202200355.
[16] I. Bassanini, S. Parapini, C. Galli, N. Vaiana, A. Pancotti, N. Basilico, D. Taramelli, S. Romeo, Discovery and pharmacophore mapping of a low-nanomolar inhibitor of p. falciparum growth, ChemMedChem 14 (2019) 1982–1994, https://doi.org/10.1002/CMDC.201900526.
[17] I. Bassanini, T. Braga, C. Tognoli, M. Vanoni, G. Mazza, N. Basilico, S. Parapini, S. Riva, A chemoenzymatic approach for the preparation of "linear-shaped" diaryl pyrazines as potential antiprotozoal agents, EurJOC 27 (2024) e202400204, https://doi.org/10.1002/ejoc.202400204.
[18] A.G. Atanasov, S.B. Zotchev, V.M. Dirsch, I. Erdogan Orhan, M. Banach, J. M. Rollinger, D. Barreca, W. Weckwerth, R. Bauer, E.A. Bayer, M. Majeed, A. Bishayee, V. Bochkov, G.K. Bonn, N. Braidy, F. Bucar, A. Cifuentes, G. Donofrio, M. Bodkin, M. Diederich, A.T. Dinkova-Kostova, T. Efferth, K. El Bairi, N. Arkells, T.-P. Fan, B.L. Fiebich, M. Freissmuth, M.I. Georgiev, S. Gibbons, K.M. Godfrey, C. W. Gruber, J. Heer, L.A. Huber, E. Ibanez, A. Kijjoa, A.K. Kiss, A. Lu, F.A. Macias, M.J.S. Miller, A. Mocan, R. Müller, F. Nicoletti, G. Perry, V. Pittalà, L. Rastrelli, M. Ristow, G. Luigi Russo, A. Sanches Silva, D. Schuster, H. Sheridan, K. Skalicka-Woźniak, L. Skaltsounis, E. Sobarzo-Sánchez, D.S. Bredt, H. Stuppner, A. Sureda, N. T. Tzvetkov, R. Anna Vacca, B.B. Aggarwal, M. Battino, F. Giampieri, M. Wink, J.-L. Wolfender, J. Xiao, A. Wai Kan Yeung, G. Lizard, M.A. Popp, M. Heinrich, I. Berindan-Neagoe, M. Stadler, M. Daglia, R. Verpoorte, C.T. Supuran, Natural products in drug discovery: advances and opportunities, Nat. Rev. Drug Discov. (2021) 200–216, https://doi.org/10.1038/s41573-020-00114-z.
[19] J. Gershenzon, N. Dudareva, The function of terpene natural products in the natural world, Nat. Chem. Biol. 3 (2007) 408–414, https://doi.org/10.1038/nchembio.2007.5.
[20] D. Tholl, Biosynthesis and biological functions of terpenoids in plants, Biotechnology of Isoprenoids (2015) 63–106, https://doi.org/10.1007/10_2014_295.
[21] F.T.G. Dereli, Plant-based bioactive components: phytochemicals: a review, Bioactive Components: A Sustainable System for Good Health and Well-Being (2022) 27–33, https://doi.org/10.1007/978-981-19-2366-1_2/TABLES/1.
[22] A. Masyita, R. Mustika Sari, A. Dwi Astuti, B. Yasir, N. Rahma Rumata, T. Bin Emran, F. Nainu, J. Simal-Gandara, Terpenes and terpenoids as main bioactive

compounds of essential oils, their roles in human health and potential application as natural food preservatives, Food Chem X 13 (2022), https://doi.org/10.1016/J.FOCHX.2022.100217.
[23] B.M. Marinho, D.N. Fernandes, M.Z. Chicoti, G.J.G. de Ribeiro, V.G. de Almeida, M.G. dos Santos, V.H.D. Guimarães, M.S. Marchioretto, H.R. Martins, G.E.B.A. de Melo, L.E. Gregorio, Phytochemical profile and antiproliferative activity of human lymphocytes of Gomphrena virgata Mart. (Amaranthaceae), Nat. Prod. Res. 36 (2022) 1641–1647, https://doi.org/10.1080/14786419.2021.1895151.
[24] A. Smelcerovic, M. Spiteller, A.P. Ligon, Z. Smelcerovic, N. Raabe, Essential oil composition of Hypericum L. species from Southeastern Serbia and their chemotaxonomy, Biochem. Syst. Ecol. 35 (2007) 99–113, https://doi.org/10.1016/j.bse.2006.09.012.
[25] H.A. Mohammed, H.M. Eldeeb, R.A. Khan, M.S. Al-Omar, S.A.A. Mohammed, M.S. M. Sajid, M.S.A. Aly, A.M. Ahmad, A.A.H. Abdellatif, S.Y. Eid, M.Z. El-Readi, Sage, salvia officinalis l., constituents, hepatoprotective activity, and cytotoxicity evaluations of the essential oils obtained from fresh and differently timed dried herbs: A comparative analysis, Molecules 26 (2021) 5757, https://doi.org/10.3390/molecules26195757.
[26] G.Y. Ji, L.C. Liu, L. Zhu, X. Xing, Chemical Composition and Antibacterial and Antioxidant Activities of the Essential Oil of Oreocharis maximowiczii, Chem. Nat. Compd. 57 (2021) 560–562, https://doi.org/10.1007/s10600-021-03416-9.
[27] A. Sulborska-Różycka, E. Weryszko-Chmielewska, B. Polak, B. Stefańczyk, A. Matysik-Woźniak, R. Rejdak, Secretory products in petals of centaurea cyanus l. flowers: a histochemistry, ultrastructure, and phytochemical study of volatile compounds, Molecules 27 (2022) 1371, https://doi.org/10.3390/molecules27041371.
[28] M. Grover T. Behl T. Virmani S. Bhatia A. Al-Harrasi L. Aleya Chrysopogon Zizanioides-a Review on Its Pharmacognosy, Chemical Composition and Pharmacological Activities 33 2021 44667 44692 10.1007/s11356-021-15145-1/ Published.
[29] F. Nagashima, S. Momosaki, Y. Watanabe, S. Takaoka, S. Huneck, Y. Asakawa, Sesquiterpenoids from the liveworts Bazzana trilobata and Porella canariensis S, Phytochemistry 42 (1996) 1361–1366.
[30] J.M. Scher, J.B. Speakman, J. Zapp, H. Becker, Bioactivity guided isolation of antifungal compounds from the liverwort Bazzania trilobata (L.) S.F. Gray, Phytochemistry 65 (2004) 2583–2588, https://doi.org/10.1016/j.phytochem.2004.05.013.
[31] G.A. Utegenova, K.B. Pallister, S.V. Kushnarenko, G. Özek, T. Özek, K. T. Abidkulova, L.N. Kirpotina, I.A. Schepetkin, M.T. Quinn, J.M. Voyich, Chemical composition and antibacterial activity of essential oils from Ferula L. species against methicillin-resistant Staphylococcus aureus, Molecules 23 (2018) 1679, https://doi.org/10.3390/molecules23071679.
[32] V. Lakshmi, K. Pandey, S.K. Agarwal, Bioactivity of the compounds in genus Dysoxylum, Acta Ecol. Sin. 29 (2009) 30–44, https://doi.org/10.1016/j.chnaes.2009.04.005.
[33] S.A. Riyadi, A.A. Naini, U. Supratman, Sesquiterpenoids from Meliaceae Family and Their Biological Activities, Molecules 28 (2023) 4874, https://doi.org/10.3390/molecules28124874.
[34] R. Mondêgo-Oliveira, J.C. de Sá Sousa, C.J. Moragas-Tellis, P.V.R. de Souza, M. S. do dos Santos Chagas, M.D. Behrens, D. de Jesús Hardoim, N.N. Taniwaki, T. Q. Chometon, A.L. Bertho, K.S. da Calabrese, F. Almeida-Souza, A.L. Abreu-Silva, Vernonia brasiliana (L.) Druce induces ultrastructural changes and apoptosis-like death of Leishmania infantum promastigotes, Biomed. Pharmacotherapy 133 (2021) 111025, https://doi.org/10.1016/j.biopha.2020.111025.
[35] L.S.S. Bosquiroli, D.P. Demarque, Y.S. Rizk, M.C. Cunha, M.C.S. Marques, M.F. C. De Matos, M.C.T. Kadri, C.A. Carollo, C.C.P. Arruda, In vitro anti-leishmania infantum activity of essential oil from piper angustifolium, Rev. Bras 25 (2015) 124–128, https://doi.org/10.1016/j.bjp.2015.03.008.
[36] C. Kauffmann, A.C. Giacomin, K. Arossi, L.A. Pacheco, L. Hoehne, E.M. de Freitas, G.M.C. de Machado, M.M.C. do Cavalheiro, S.C.B. Gnoatto, E.M. Ethur, Antileishmanial in vitro activity of essential oil from myrciaria plinioides, a native species from Southern Brazil, Braz. J. Pharm. Sci. 55 (2019), https://doi.org/10.1590/s2175-97902019000217584.
[37] A.M. Alhassan, Q.U. Ahmed, I. Malami, Z.A. Zakaria, Pseudocedrela kotschyi: a review of ethnomedicinal uses, pharmacology and phytochemistry, Pharm. Biol. 59 (2021) 955–963, https://doi.org/10.1080/13880209.2021.1950776.
[38] I.A. Rodrigues, M.M.B. Azevedo, F.C.M. Chaves, H.R. Bizzo, S. Corte-Real, D. S. Alviano, C.S. Alviano, M.S.S. Rosa, A.B. Vermelho, In vitro cytocidal effects of the essential oil from Croton cajucara (red sacaca) and its major constituent 7-hydroxycalamenene against Leishmania chagasi, BMC Complement. Altern. Med. 13 (2013) 1–9, https://doi.org/10.1186/1472-6882-13-249/FIGURES/5.
[39] S. Afoulous, H. Ferhout, E.G. Raoelison, A. Valentin, B. Moukarzel, F. Couderc, J. Bouajila, Helichrysum gymnocephalum essential oil: chemical composition and cytotoxic, antimalarial and antioxidant activities, attribution of the activity origin by correlations, Molecules 16 (2011) 8273–8291, https://doi.org/10.3390/molecules16108273.
[40] M. Nishizawa, H. Yamada, S. Setijati, H. Yuji, Structure and synthesis of bicalamenene, TetrahedronLett 26 (1985) 1535–1536.
[41] S. Faisal, S.L. Badshah, B. Kubra, A.H. Emwas, M. Jaremko, Alkaloids as potential antivirals. a comprehensive review, Nat Prod Bioprospect 13 (2023) 3–38, https://doi.org/10.1007/s13659-022-00366-9.
[42] C.T. Zi, L. Yang, F.Q. Xu, F.W. Dong, D. Yang, Y. Li, Z.T. Ding, J. Zhou, Z.H. Jiang, J.M. Hu, Synthesis and anticancer activity of dimeric podophyllotoxin derivatives, Drug Des. Devel. Ther. 12 (2018) 3393–3406, https://doi.org/10.2147/DDDT.S167382.
[43] I. Lopes, C. Campos, R. Medeiros, F. Cerqueira, Antimicrobial Activity of Dimeric Flavonoids, Compounds 4 (2024) 214–229, https://doi.org/10.3390/compounds4020011.
[44] M. Ogata, Antioxidant and antibacterial activities of dimeric phenol compounds, Yakugaku Zasshi 128 (2008) 1147–1158, https://doi.org/10.1248/YAKUSHI.128.1149.
[45] R.C. Cambie, A.R. Lal, F. Ahmad, Sesquiterpenes from heritiera ornithocephala, Phytochemistry 29 (1990) 2329–2331.
[46] H. El-Seedi, F. Ghia, K.B.G. Torssell, Cadinane Sesquiterpenes from Siparuna macrotepala, Phytochemistry 35 (1994) 1495–1497.
[47] S. Serra, C. Fuganti, Aromatic annulation on the p-menthane monoterpenes: Enantiospecific synthesis of the trans and cis isomers of calamenene and 8-hydroxycalamenene, Tetrahedron Lett. 46 (2005) 4769–4772, https://doi.org/10.1016/j.tetlet.2005.05.037.
[48] S. Serra, C. Fuganti, E. Brenna, Recent advances in the benzannulation of substituted 3-alkoxycarbonyl-3,5-hexadienoic acids and 3-alkoxycarbonylhex-3-en-5-ynoic acids to polysubstituted aromatics, Chemistry 13 (2007) 6782–6791, https://doi.org/10.1002/CHEM.200700735.
[49] S. Riva, Laccases: blue enzymes for green chemistry, Trends Biotechnol. 24 (2006) 219–226, https://doi.org/10.1016/j.tibtech.2006.03.006.
[50] I. Bassanini, E.E. Ferrandi, S. Riva, D. Monti, Biocatalysis with laccases: An updated overview, Catalysts 11 (2021) 1–30, https://doi.org/10.3390/catal11010026.
[51] S. Ncanana, L. Baratto, L. Roncaglia, S. Riva, S.G. Burton, Laccase-mediated oxidation of totarol, Adv. Synth. Catal. 349 (2007) 1507–1513, https://doi.org/10.1002/adsc.200700005.
[52] L.J. Mitchell, C.J. Moody, Solar photochemical oxidation of alcohols using catalytic hydroquinone and copper nanoparticles under oxygen: Oxidative cleavage of lignin models, J. Org. Chem. 79 (2014) 11091–11100, https://doi.org/10.1021/JO5020917/SUPPL_FILE/JO5020917_SI_001.PDF.
[53] M. Bonomi, G. Bussi, C. Camilloni, G.A. Tribello, P. Banáš, A. Barducci, M. Bernetti, P.G. Bolhuis, S. Bottaro, D. Branduardi, R. Capelli, P. Carloni, M. Ceriotti, A. Cesari, H. Chen, W. Chen, F. Colizzi, S. De, M. De La Pierre, D. Donadio, V. Drobot, B. Ensing, A.L. Ferguson, M. Filizola, J.S. Fraser, H. Fu, P. Gasparotto, F. L. Gervasio, F. Giberti, A. Gil-Ley, T. Giorgino, G.T. Heller, G.M. Hocky, M. Iannuzzi, M. Invernizzi, K.E. Jelfs, A. Jussupow, E. Kirilin, A. Laio, V. Limongelli, K. Lindorff-Larsen, T. Löhr, F. Marinelli, L. Martin-Samos, M. Masetti, R. Meyer, A. Michaelides, C. Molteni, T. Morishita, M. Nava, C. Paissoni, E. Papaleo, M. Parrinello, J. Pfaendtner, P. Piaggi, G.M. Piccini, A. Pietropaolo, F. Pietrucci, S. Pipolo, D. Provasi, D. Quigley, P. Raiteri, S. Raniolo, J. Rydzewski, M. Salvalaglio, G.C. Sosso, V. Spiwok, J. Šponer, D.W.H. Swenson, P. Tiwary, O. Valsson, M. Vendruscolo, G.A.A. Voth, Promoting transparency and reproducibility in enhanced molecular simulations, Nat. Methods 16 (8) (2019) 670–673, https://doi.org/10.1038/s41592-019-0506-8.
[54] D.A.; Case, H.M.; Aktulga, K.; Belfon, I.Y.; Ben-Shalom, J.T.; Berryman, S.R.; Brozell, D.S.; Cerutti, T.E.; Cheatham, G.A.; Cisneros, V.W.D.; Cruzeiro, T.A.; Darden, N.; Forouzesh, M.; Ghazimirsaeed, G.; Giambasu, T.; Giese, M.K.; Gilson, H.; Gohlke, A.W.; Goetz, J.; Harris, Z.; Huang, S.; Izadi, S.A.; Izamailov, K.; Kasavajhala, M.C.; Kayamak, A.; Kovalenko, T.; Kurtzman, T.S.; Lee, P.; Li, Z.; Li, C.; Li, J.; Lin, J.; Liu, T.; Luchko, R.; Luo, M.; Machado, M.; Manathunga, K.M.; Merz, Y.; Miao, O.; Mikhailovskii, G.; Monard, H.; Nguyen, K.A.; O'Hean, A.; Onufriev, F.; Pan, S.; Pantano, A.; Rahnamoun, D.R.; Roe, A.; Roitberg, C.; Sagui, S.; Schott-Verdugo, A.; Shajan, J.; Shen, C.L.; Simmerling, N.R.; Sjrynnkov, J.; Smith, J.; Swails, R.C.; Walker, J.; Wang, J.; Wang, X.; Wu, Y.; Xiong, Y.; Xue, D.M.; York, C. Zhao;, Q.; Zhu, P.A. Kollman, Amber - University of California (San Francisco), 2024.
[55] D.A. Case, H.M. Aktulga, K. Belfon, D.S. Cerutti, G.A. Cisneros, V.W.D. Cruzeiro, N. Forouzesh, T.J. Giese, A.W. Götz, H. Gohlke, S. Izadi, K. Kasavajhala, M. C. Kaymak, E. King, T. Kurtzman, T.S. Lee, P. Li, J. Liu, T. Luchko, R. Luo, M. Manathunga, M.R. Machado, H.M. Nguyen, K.A. O'Hearn, A.V. Onufriev, F. Pan, S. Pantano, R. Qi, A. Rahnamoun, A. Risheh, S. Schott-Verdugo, A. Shajan, J. Swails, J. Wang, H. Wei, X. Wu, Y. Wu, S. Zhang, S. Zhao, Q. Zhu, T.E. Cheatham, D.R. Roe, A. Roitberg, C. Simmerling, D.M. York, M.C. Nagan, K.M. Merz, Ambertools, J. Chem. Inf. Model. 63 (2023) 6183–6191, https://doi.org/10.1021/ACS.JCIM.3C01153/ASSET/IMAGES/LARGE/CI3C01153_0002.JPEG.
[56] S. Jo, T. Kim, V.G. Iyer, W. Im, CHARMM-GUI: a web-based graphical user interface for CHARMM, J. Comput. Chem. 29 (2008) 1859–1865, https://doi.org/10.1002/JCC.20945.
[57] S.J. Park, N. Kern, T. Brown, J. Lee, W. Im, CHARMM-GUI PDB manipulator: various PDB structural modifications for biomolecular modeling and simulation, J. Mol. Biol. 435 (2023) 167995, https://doi.org/10.1016/J.JMB.2023.167995.
[58] S. Jo, X. Cheng, S.M. Islam, L. Huang, H. Rui, A. Zhu, H.S. Lee, Y. Qi, W. Han, K. Vanommeslaeghe, A.D. MacKerell, B. Roux, W. Im, CHARMM-GUI PDB manipulator for advanced modeling and simulations of proteins containing nonstandard residues, Adv. Protein Chem. Struct. Biol. 96 (2014) 235–265, https://doi.org/10.1016/BS.APCSB.2014.06.002.
[59] Package "cuda.ml" Title R Interface for the RAPIDS cuML Suite of Libraries, (2022).
[60] D. Cremer, J.A. Pople, A general definition of ring puckering coordinates, J. Am. Chem. Soc. 97 (1975) 1354–1358, https://doi.org/10.1021/JA00839A011/ASSET/JA00839A011.FP.PNG_V03.
[61] X. Biarnés, A. Ardèvol, A. Planas, C. Rovira, A. Laio, M. Parrinello, The conformational free energy landscape of β-D-glucopyranose. implications for substrate preactivation in β-glucoside hydrolases, , J Am Chem Soc 129 (2007) 10686–10693, https://doi.org/10.1021/JA068411O/SUPPL_FILE/JA068411OSI20070705_061349.PDF.

[62] R Core TEAM, R: A Language and Environment for Statistical Computing - R Foundation for Statistical Computing: Vienna, Austria, n.d.
[63] Y. Li, D. Falbel, Cuda.Ml: R Interface for the RAPIDS cuML Suite of Libraries, 2022.
[64] C. Adamo, V. Barone, Toward reliable density functional methods without adjustable parameters: The PBE0 model, J. Chem. Phys. 110 (1999) 6158–6170, https://doi.org/10.1063/1.478522.
[65] L.A. Curtiss, M.P. McGrath, J.P. Blaudeau, N.E. Davis, R.C. Binning, L. Radom, Extension of Gaussian-2 theory to molecules containing third-row atoms Ga–Kr, J. Chem. Phys. 103 (1995) 6104–6113, https://doi.org/10.1063/1.470438.
[66] A. Robb J.R. Cheeseman G. Scalmani V. Barone V.G.A. Petersson H. Nakatsuji X. Li M. Caricato A.V. Marenich J. Bloino B.G. Janesko R. Gomperts B. Mennucci H.P. Hratchian J.V. Ortiz A.F. Izmaylov J.L. Sonnenberg D. Williams-Young F.F. Ding F. Lipparini J. Egidi B. Goings A. Peng T. Petrone D. Henderson V.G. Ranasinghe J. Zakrzewski N. Gao G. Rega W. Zheng M. Liang M. Hada K. Ehara R. Toyota J. Fukuda M. Hasegawa T. Ishida Y. Nakajima O. Honda H. Kitao T. Nakai K. Vreven J.A. Throssell J.E. Montgomery F. Peralta M.J. Ogliaro J.J. Bearpark E.N. Heyd K. N. Brothers V.N. Kudin T.A. Staroverov R. Keith J. Kobayashi K. Normand A.P. Raghavachari J.C. Rendell S.S. Burant J. Iyengar M. Tomasi J.M. Cossi M. Millam C. Klene R. Adamo J.W. Cammi R.L. Ochterski K. Martin O. Morokuma J.B. Farkas D.J.F. Foresman Gaussian 16, Revision C.01 Gaussian Inc 2016 Wallingford CT.
[67] J. Tomasi, B. Mennucci, R. Cammi, Quantum mechanical continuum solvation models, Chem. Rev. 105 (2005) 2999–3093, https://doi.org/10.1021/CR9904009/ASSET/IMAGES/MEDIUM/CR9904009E00087.GIF.
[68] T. Bruhn, A. Schaumlöffel, Y. Hemberger, G. Bringmann, SpecDis: quantifying the comparison of calculated and experimental electronic circular dichroism spectra, Chirality 25 (2013) 243–249, https://doi.org/10.1002/CHIR.22138.
[69] G. Pescitelli, T. Bruhn, Good computational practice in the assignment of absolute configurations by TDDFT calculations of ECD Spectra, Chirality 28 (2016) 466–474, https://doi.org/10.1002/CHIR.22600.
[70] W. Trager, J.B. Jensen, Human malaria parasites in continuous culture, Science 193 (1976) (1979) 673–675, https://doi.org/10.1126/SCIENCE.781840.
[71] S. D'Alessandro, M. Gelati, N. Basilico, E.A. Parati, R.K. Haynes, D. Taramelli, Differential effects on angiogenesis of two antimalarial compounds, dihydroartemisinin and artemisone: Implications for embryotoxicity, Toxicology 241 (2007) 66–74, https://doi.org/10.1016/J.TOX.2007.08.084.
[72] I. Bassanini, P. Gavezzotti, D. Monti, J. Krejzová, V. Křen, S. Riva, Laccase-catalyzed dimerization of glycosylated lignols, J. Mol. Catal. B Enzym. 134 (2016) 295–301, https://doi.org/10.1016/j.molcatb.2016.10.019.
[73] P. Gavezzotti, F. Bertacchi, G. Fronza, V. Křen, D. Monti, S. Riva, Laccase-catalyzed dimerization of piceid, a resveratrol glucoside, and its further enzymatic elaboration, Adv. Synth. Catal. 357 (2015) 1831–1839, https://doi.org/10.1002/adsc.201500185.
[74] S. Ficarra, E. Tellone, D. Pirolli, A. Russo, D. Barreca, A. Galtieri, B. Giardina, P. Gavezzotti, S. Riva, M.C. De Rosa, Insights into the properties of the two enantiomers of trans-δ-viniferin, a resveratrol derivative: antioxidant activity, biochemical and molecular modeling studies of its interactions with hemoglobin, Mol. Biosyst. 12 (2016) 1276–1286, https://doi.org/10.1039/C5MB00897B.
[75] P. Gavezzotti, E. Vavříková, G. Fronza, T. Kudanga, M. Kuzma, S. Riva, D. Biedermann, V. Křen, Enzymatic oxidative dimerization of silymarin flavonolignans, J. Mol. Catal. B Enzym. 109 (2014) 24–30, https://doi.org/10.1016/j.molcatb.2014.07.012.
[76] G. Bringmann, T. Bruhn, K. Maksimenka, Y. Hemberger, The assignment of absolute stereostructures through quantum chemical circular dichroism calculations, European J Org Chem (2009) 2717–2727, https://doi.org/10.1002/EJOC.200801121.
[77] M. Górecki, V. Zullo, A. Iuliano, G. Pescitelli, On the absolute stereochemistry of tolterodine: a circular dichroism study, Pharmaceuticals 12 (2019) 21, https://doi.org/10.3390/PH12010021.
[78] M. Sharifi Tabar, C. Parsania, H. Chen, X.D. Su, C.G. Bailey, J.E.J. Rasko, Illuminating the dark protein-protein interactome, Cell Reports Methods 2 (2022) 100275, https://doi.org/10.1016/j.crmeth.2022.100275.
[79] K. Atz, L. Cotos, C. Isert, M. Håkansson, D. Focht, M. Hilleke, D.F. Nippa, M. Iff, J. Ledergerber, C.C.G. Schiebroek, V. Romeo, J.A. Hiss, D. Merk, P. Schneider, B. Kuhn, U. Grether, G. Schneider, Prospective de novo drug design with deep interactome learning, Nat. Commun. 15 (2024) 3408, https://doi.org/10.1038/s41467-024-47613-w.